

# **PERFORMANCE ASSESSMENT OF GEOCELL REINFORCED FLEXIBLE PAVEMENTS**

KAPIL DHAWAN

CE15MTECH11007

A Dissertation Submitted to  
Indian Institute of Technology Hyderabad  
In Partial Fulfillment of the Requirements for  
The Degree of Master of Technology



भारतीय प्रौद्योगिकी संस्थान हैदराबाद  
Indian Institute of Technology Hyderabad

Department of Civil Engineering

June, 2017

## Declaration

I declare that this written submission represents my ideas in my own words, and where others ideas or words have been included, I have adequately cited and referenced the original sources. I also declare that I have adhered to all principles of academic honesty and integrity and have not misrepresented or fabricated or falsified any idea/data/fact/source in my submission. I understand that any violation of the above will be a cause for disciplinary action by the Institute and can also evoke penal action from the sources that have thus not been properly cited, or from whom proper permission has not been taken when needed.



Signature

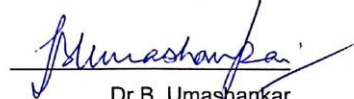
(KAPIL DHAWAN)  
CE15MTECH11007

## Approval Sheet

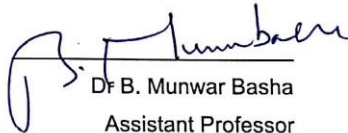
This thesis entitled "Performance Assessment of Geocell Reinforced Flexible Pavements" by Kapil Dhawan is approved for the degree of Master of Technology from IIT Hyderabad.



Dr S. Sireesh  
Associate Professor  
Department of Civil Engineering  
Indian Institute of Technology Hyderabad



Dr B. Umashankar  
Associate Professor  
Head of the Department  
Department of Civil Engineering  
Indian Institute of Technology Hyderabad



Dr B. Munwar Basha  
Assistant Professor  
Department of Civil Engineering  
Indian Institute of Technology Hyderabad



Dr. R. Prasanth Kumar  
Associate Professor  
Department of Mechanical and Aerospace Engineering  
Indian Institute of Technology Hyderabad

## **Acknowledgements**

My sincere gratitude to my advisor Dr. S. Sireesh for his continuous support, help, and motivation. I would also like to thank all the other faculty members of Civil Engineering Department, IITH.

I am grateful to my Parents for their invaluable motivation to complete my M. Tech Thesis.

My heartfelt thanks to my classmates Rohith, Arvind, Shellas, Soujanya, and Tejaswi.

I would like to thank my seniors Pranav, Vinay, Mahesh for clearing my doubts and for being supportive all through the days.

KAPIL DHAWAN

**Dedicated**

**To**

**My Parents**

## **Abstract**

The influence of introducing a three dimensional geo-synthetic material, called geocells in the base layer of flexible pavements is investigated in the current study. This study compares the reinforced and unreinforced pavement sections constructed on a subgrade having a moderate California bearing ratio (CBR) value of 5%. A series of model tests were carried out to understand the influence of geocell reinforcement on the load carrying mechanism of the pavement section under static and repeated loading conditions. The parameters studied were as follows: load-settlement response of the pavement sections, actual rut at the subgrade level, pressure transmitted to the subgrade soil underlying the geocell reinforced base layer and surface deformation profile of the test sections.

Different flexible pavement design methodologies proposed by Indian Roads Congress (IRC) and American Association of State Highways and Transportation Officials (AASHTO) were used for the design of pavement sections and were compared through experimental program conducted in the laboratory. Large scale repeated load tests were performed to replicate the actual field conditions. The test results indicate that the geocell reinforcement reduces the rutting in the pavement. The performance improvement was presented in terms of traffic benefit ratios (TBR), layer coefficient ratios (LCR), rut depth reductions (RDR) and rut benefit ratios (RBR). Besides, under the same load repetitions, the thickness of the reinforced pavement is considerably less than that of the unreinforced pavement section. In addition to the cost savings, this would conserve natural materials like aggregates used in the pavement construction. Overall, the inclusion of geocell in the base layer helps in improving the life, uniform distribution of load, reduction in rut depth and it also provides an economical and sustainable solution to the present practices.

# Nomenclature

LL – Liquid limit

PL – Plastic limit

OMC – Optimum moisture content

MDD – Maximum dry density

CBR – California bearing ratio

PG – Penetration Grade

WMM – Wet mix macadam

MORTH – Ministry Of Road Transport and Highways

IRC – Indian Road Congress

IS – Indian Standards

AASHTO – American Association of State Highway and Transport Officials

LVDT – Linear variable displacement transducer

D – Diameter of the loading plate

h – Height of geocell

b – Width of geocell

CPD – Cumulative permanent deformation

$CPD_{rein}$  – Cumulative permanent deformation in reinforced test section

$CPD_{unrein}$  – Cumulative permanent deformation in unreinforced test section

MPT – Multi Purpose test ware

DAQ – Data acquisition system

TBR – Traffic benefit ratio

RDR – Rut depth reduction

RBR – Rut benefit ratio

EMIF – Equivalent Modulus Improvement Factor

LCR – Layer Coefficient Ratio

$E_{reinf}$  – Total elastic modulus of the reinforced pavement section

$E_{unreinf}$  – Total elastic modulus of the unreinforced pavement section

$N_r$  – No. of cycles required to reach a given amount of rut depth in reinforced test section

$N_u$  – No. of cycles required to reach a given amount of rut depth in unreinforced test section

$M_r$  – Resilient modulus

SN – Structural number



## Contents

Declaration.....	<b>Error! Bookmark not defined.</b>
Acknowledgements.....	ii
Abstract.....	iv
Chapter 1 Introduction.....	1
1.1 General.....	1
1.2 Geocell.....	2
1.3 Geocell-reinforced Granular Bases.....	2
1.4 Objectives of the study.....	3
1.5 Research Methodology.....	4
1.6 Thesis outline.....	4
Chapter 2 Literature Review.....	5
2.1 Introduction.....	5
2.2 Studies on Geocell reinforcement under static load.....	5
2.3 Studies on geocell reinforcement under repeated load.....	7
2.4 Studies on designing pavements with geo-synthetics.....	8
2.5 Summary.....	9
Chapter 3 Materials and Methods.....	11
3.1 Introduction.....	11
3.2 Characteristics of subgrade soil.....	11
3.2.1 Sieve analysis.....	11
3.2.2 Atterberg's limits.....	12
3.2.3 Specific gravity.....	12
3.2.4 Compaction characteristics.....	14
3.2.5 California Bearing Ratio.....	15
3.3 Characteristics of Wet Mix Macadam (WMM).....	17
3.3.1 Compaction characteristics.....	17

3.4 Characteristics of Geocell .....	18
3.5 Characteristics of bituminous course (BC) layer .....	19
3.6 Test methodology.....	20
3.6.1 Test setup .....	20
3.6.2 Preparation of test beds .....	21
3.6.3 Data acquisition system and instrumentation.....	23
3.6.4 Test procedure.....	25
3.7 Performance indicators .....	27
3.7.1 Cumulative permanent deformations .....	27
3.7.2 Traffic benefit ratio .....	27
3.7.3 Rut depth reduction.....	28
3.7.4 Equivalent modulus improvement factor .....	28
3.7.5 Rut benefit ratio .....	28
3.7.6 Layer coefficient ratio.....	29
3.8 Summary .....	29
Chapter 4 Results and Discussion.....	30
4.1 Introduction.....	30
4.2 Design approach.....	30
4.2.1 Verifying the results of IRC using AASHTO (1993) .....	33
4.2.2 AASHTO design method through TBR approach (reinforced pavement section) [41] .....	34
4.2.3 AASHTO design through LCR approach (reinforced pavement section) .....	36
4.3 Equivalent modulus improvement factor .....	37
4.4 Static load test results.....	38
4.5 Repetitive load test results .....	43
4.5.1 Traffic benefit ratio .....	45
4.5.2 Rut depth reduction.....	45
4.5.3 Subgrade deformation .....	46
4.5.4 Rut benefit ratio .....	47
4.6 Cost analysis .....	51

4.7 Summary.....	51
Chapter 5 Conclusion.....	52
References.....	53

## LIST OF FIGURES

Figure 1.1 Varieties of geo-synthetics used in pavements [1] .....	2
Figure 1.2 fLoading mechanism of geocell reinforced bases (Biabani et al. 2016) [4] .....	3
Figure 1.3 Load transfer mechanism of geocell mattress (Kim et al.,2013) [5] .....	3
Figure 2.1 Variation of LCR with subgrade CBR [30] .....	9
Figure 2.1 Estimate of LCR for Design based on Performance at 25 mm Permanent Deflection [31] ..	9
Figure 3.1 Sieve analysis of the subgrade soil .....	12
Figure 3.2a Images of the LL and PL test.....	13
Figure 3.2b Flow curve of clayey soil.....	13
Figure 3.3 Specific gravity test by density bottle method.....	14
Figure 3.4 Mold and hammer used in standard proctor test.....	14
Figure 3.5 Compaction characteristics of the subgrade soil .....	15
Figure 3.6a CBR setup and posttest specimen .....	16
Figure 3.6b Load-settlement curve for CBR test .....	16
Figure 3.7 Compaction characteristics of the Wet Mix Macadam layer.....	18
Figure 3.8 Typical geocell used in the study .....	19
Figure 3.9 Large scale test setup.....	20
Figure 3.10 Calibration curve for subgrade .....	21
Figure 3.11 A typical section shows the different layers .....	23
Figure 3.12 Various stages for the preparation of the test section .....	23
Figure 3.13 DAQ Systems MX 840 and MX 1615.....	24
Figure 3.14 Typical close-loop control program in MPT software .....	25
Figure 3.15 Typical loading patterns (a) for static test (b) repeated load test.....	26
Figure 3.16 Elastic and plastic strains of a typical loading cycle .....	27
Figure 4.1 Locations of critical strains.....	31
Figure 4.2 Typical pavement design chart for subgrade CBR of 5% (IRC 37:2012) .....	32
Figure 4.3 Pressure-settlement curve for 440mm thick base geocell reinforced and unreinforced test sections.....	37
Figure 4.4 Unreinforced test section used in the study .....	39
Figure 4.5 Reinforced test section used in the study.....	39
Figure 4.6 Pressure-settlement curve for 440mm thick unreinforced and 250mm thick base geocell reinforced test sections.....	40
Figure 4.7 Surface deformation profile of unreinforced test section .....	41
Figure 4.8 Surface deformation profile of reinforced test section (250mm base) .....	42
Figure 4.9 Pressure acting on the subgrade at different loads applied (Unreinforced).....	42

Figure 4.10 Pressure acting on the subgrade at different loads applied (Reinforced 250mm base) .....	43
Figure 4.11 Variation of cumulative plastic deformations with no. of load repetitions .....	44
Figure 4.12 Variation of TBR with respect to CPD.....	45
Figure 4.13 Shows the variation of RDR with no. of loading cycles.....	46
Figure 4.14 Variation of rut depth with the no. of load cycles .....	47
Figure 4.15 Variation of RBR with number of cycles .....	48
Figure 4.16 Surface deformation profile for unreinforced case .....	48
Figure 4.17 Surface deformation profile of reinforced test section (250mm) .....	49
Figure 4.18 Variation of contact pressure measured at the base-subgrade interface for geocell reinforced test section (250mm) .....	50
Figure 4.19 Variation of contact pressure measured at the base-subgrade interface for geocell reinforced test section (250 mm) .....	50

## LIST OF TABLES

Table 2.1 Summary of studies performed on geocell mattress under static loading condition.....	6
Table 2.2 Summary of studies performed on design of geo-synthetic reinforced pavements .....	7
Table 2.3 Summary of studies performed on design of geo-synthetic reinforced pavements .....	8
Table 3.1 Grading requirements of aggregates for Wet Mix Macadam.....	17
Table 3.2 Grading requirements of aggregates for bitumen Layer .....	19
Table 4.1 Results from AASHTO method .....	33
Table 4.2 Comparison of the results .....	33
Table 4.3 Comparison of the strains developed and limiting strains .....	34
Table 4.4 Reinforced pavement design .....	36
Table 4.5 Test summary.....	38
Table 4.6 Cost analysis of a km stretch of unreinforced flexible pavement .....	51
Table 4.7 Cost analysis of a km stretch of geocell reinforced flexible pavement.....	51

# Chapter 1

## Introduction

### 1.1 General

Constant increases in traffic frequency and axle loads place great demands on the existing road network. The stresses induced between layers soon result in crack formation, and any local differential settlements may lead to subsequent settlement of upper layers. These stresses results in crack formation in surface layer i.e. fatigue and the settlement by local differential settlement i.e. rutting. The nature of soil present around the world are of many varieties ranging from dense to very loose and stiff to very weak. Since the availability of good construction site is limited, in spite of how weak the soil is, there is need to improve such sites when it is not possible to avoid such sites. For the past few decades, use of geo-synthetics has been gaining advantages over the other improvement methods especially in pavement industry. Recently the application of geocells in pavement layers have been showing much performance improvement as it can provide an additional lateral confinement to the infill material over and above the reinforcement functions provided by conventional geo-synthetics. Several research studies have shown in the past that the geocell reinforcement is effective when a granular infill is used over weak subgrades under monotonic loading conditions. Studies were performed on the flexible pavements with and without geocell reinforced basal layer under static and repeated loading. However, not much information is reported in the literature on repeated load tests on pavement sections reinforced with geocells with extensive instrumentation. Hence, there is a need to understand the behavior of geocell reinforced granular aggregate bases over weak subgrades under repetitive traffic loading. Rutting is a common phenomenon encountered in flexible pavements supported by weak subgrades. Reinforcing the weak subgrades is one of the promising alternatives to counter the pavement surface rutting. Reduction in rut depth can be achieved using Geocell in the bases of flexible pavements. Studies have proved that inclusion of basal geocells can reduce rut depth to a greater extent. Studies have shown that geocell can be used for soil confinement to provide additional strength and stiffness to the base course. Fig. 1.1 shows different types of geo-synthetics useful for pavements.

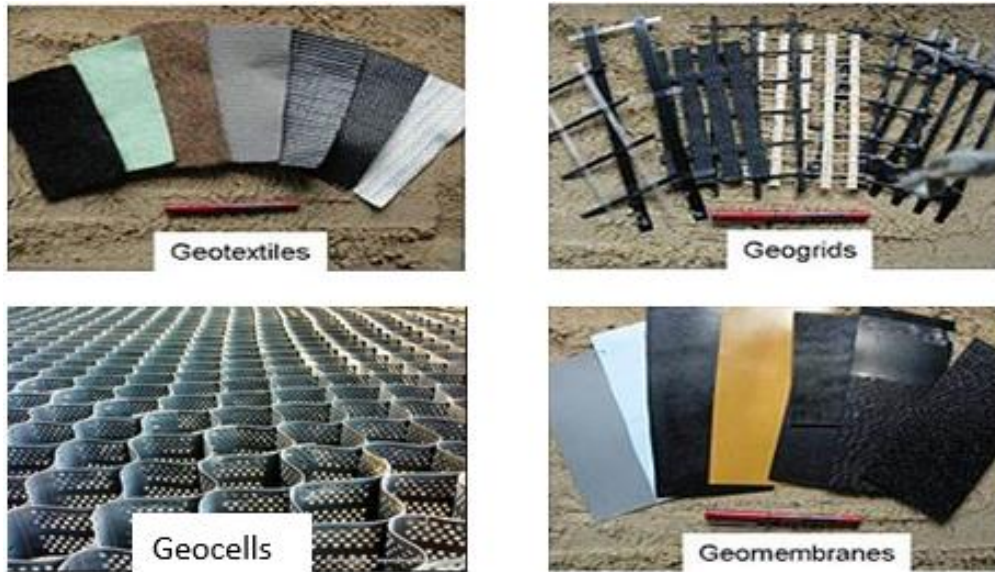


**Figure 1.1 Varieties of geo-synthetics used in pavements [1]**

## **1.2 Geocell**

The concept of lateral confinement by cellular structures dates back to 1970s. The United States Army Corps of Engineers developed this idea for providing lateral confinement to improve the bearing capacity of poorly graded sand (Webster, 1981) [2]. The predecessors of present geocells were sand grids made up of paper soaked in phenolic water resistant resin. Later, metallic geocells, especially those made of aluminum, were chosen because of strength requirements, but they proved unfeasible because of handling difficulty and high cost. Geocells have also been made using geo-grid sheets jointed by bodkin bars (for example, Carter and Dixon, 1995 [3]). At present, high-density polyethylene (HDPE) is the common polymer used to make geocells by welding extruded HDPE strips together to form honeycombs. Several research studies have shown in the past that the geocell reinforcement is effective when a granular infill is used over weak subgrades under monotonic loading conditions.

## **1.3 Geocell reinforced Granular Bases**

Nowadays geocells are extensively used in base layers to restrict the lateral spreading of the material caused due to the movement of traffic. The geocell reinforcement provides a confinement to the infill material. The typical section consists of a moderate subgrade, a geocell-reinforced granular base, and a surface layer. The replication of traffic load from the axles is done with the help of repeated load test in which a load equivalent to a contact pressure of 550kPa is applied. The study is done to analyze the rutting behavior of geocell reinforced pavements with reduced thickness and analyzing the pressure distribution through it. Properties of geocell reinforced bases, and the interaction of geocell with the material contributing to the vertical and horizontal confinement characterize the overall



behavior of the reinforced composite section. The inclusion of three dimensional geocell structure as basal reinforcement has been found to be effective in lateral confinement. Past research showed that geocell reinforcement at the base course of an unpaved road improves the engineering behavior of the reinforced composite section, such as stiffness and bearing capacity.

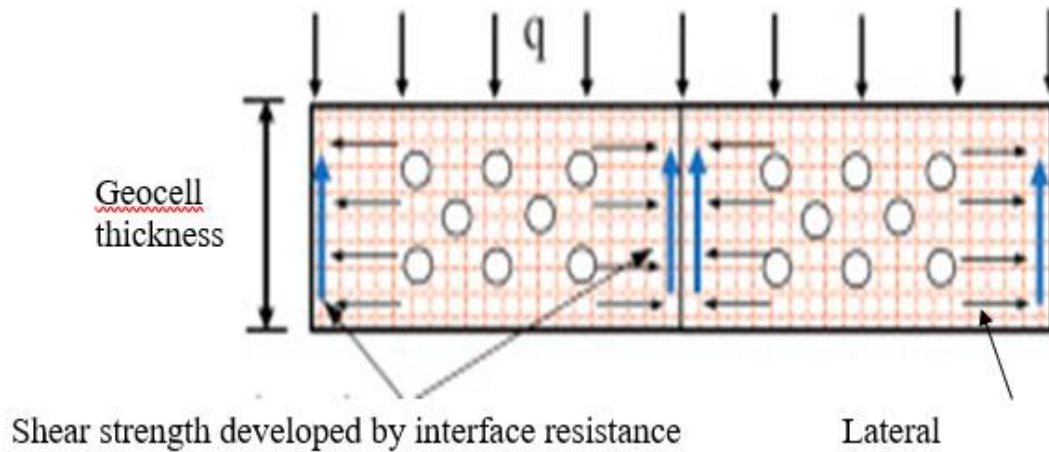


**Figure 1.2 Loading mechanism of geocell reinforced bases (Biabani et al.) [4]**

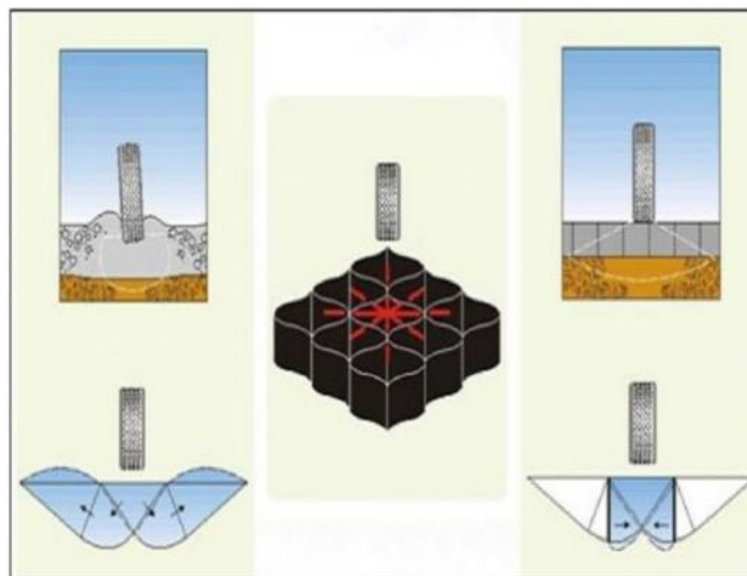


**Figure 1.3 Load transfer mechanism of geocell mattress (Kim et al.) [5]**

## 1.4 Objectives of the study

The objectives of this study are

1. To verify the pavement design procedures (IRC and AASHTO) through experimental program.
2. To replicate the actual field conditions in the lab by conducting large scale tests.
3. To study the rutting behavior of geocell reinforced pavement.

4. To reduce the usage of conventional materials which are very scarce in nature.

## **1.5 Research Methodology**

This research was conducted by adopting the following methodologies: (1) an extensive literature review on geo-synthetic reinforced bases in unpaved roads with an emphasis on geocell reinforcement including load transfer mechanisms and influence factors; (2) large scale testing of geocell-reinforced bases under static and repeated loads to evaluate the effect of geocell reinforcement and its influence factors; (3) verifying the pavement design procedures with the experimental program using large scale tests conducted at the IIT Hyderabad.

## **1.6 Thesis outline**

**Chapter 1** describes the advantages of pavement reinforcement with geocells. The design procedures available for reinforced pavements are also discussed. It also describes the objectives of the present work and the purpose of various chapters and their contents.

**Chapter 2** reviews the literature available on geo-synthetic reinforcement of pavement layers and its impact on performance of pavement. The importance of various performance indicators presented by researchers and the design procedures followed are discussed.

**Chapter 3** describes the details of various materials used and test procedures adopted in this study.

**Chapter 4** summarizes the test results of large scale testing on prepared flexible pavement beds with and without geocell reinforcement. Design of reinforced flexible pavements as per IRC and AASHTO method are compared and verified for safety against rutting and fatigue. Finally conclusions drawn from the study are presented.

**Chapter 5** presents the conclusions drawn from the study.

# Chapter 2

## Literature Review

### 2.1 Introduction

This chapter deals with the work carried out by various practitioners and researchers on the geo-synthetic reinforced soil and pavement structures under static and repeated traffic loading. The main emphasis was to study the behavior of geocell reinforced pavements under varying load conditions. Important studies on geocells are included as the primary aim of this study is to understand the behavior of geocell mattress under different loading conditions.

Many researchers studied the possible use of geo-synthetics such as geo-grids, geo-nets, geo-textiles, composites and geocells in pavement layers as a reinforcement in low volume roads to reduce the possible effect of rutting phenomenon (Giroud & Noiray [6]; Barker [7]; Haas et al. [8]; Al-Qadi et al. [9]). Generally, the bearing capacity improvement factor and traffic benefit ratio (TBR) are employed as the performance indicators for the geo-synthetic reinforced foundations and pavement structures for static and repetitive loads, respectively. The TBR can be defined as a ratio of number of load repetitions applied on the reinforced beds to the number of load repetitions applied on the unreinforced bed for a given rut depth.

### 2.2 Studies on Geocell reinforcement under static load

The studies on a 3-dimensional reinforcing structure named geocell was introduced considering the additional function of confinement along with the various functions provided by planar geo-synthetics like geo-grids and geo-textiles. Bush et al. [10] carried work on the design and construction of geocell foundation mattress supporting embankments over soft grounds. They concluded that the differential and total settlements were reduced due to load distribution through geocell mattress. The study also reported that the cost saving up to 30% can be achieved by constructing geocell reinforced embankment over soft soil as compared to conventional methods. Several researchers (Barksdale [11]; Cowland and Wong [12]; Cancelli, [13]; Collin [14], Dash et al. [15]; Sitharam and Sireesh, [16]) have done extensive study on the geocell reinforced beds under static loading conditions to understand the behavior of geocell mattress and have successfully quantified the improvements mainly in terms of increased bearing capacity of footing. Saride et al. [17] and Han et al. [18] reported that the geocell reinforcement proved effective in increasing the bearing capacity of footings because of the lateral confinement of the cell in case of a geocell under static loadings. It was observed that the placement of geocell from the surface of loading is also an important factor in improving the

performance of reinforced beds. Studies performed by Dash et al [19] and Sitharam and Sireesh [16] suggested that the placement depth of geocell should be maintained about 1 to 5% of the width of the loading area in static load tests. Dash et al. [19] performed model studies on circular footing supported on geocell reinforced sand placed on soft clay subgrades and concluded that the performance of the test beds can be improved drastically by employing geocells in a dense sand layers. They also observed about 80% reduction in footing settlements when an optimum size of geocell (width ratio,  $b/D = 5$  and height ratio,  $h/D = 2.1$ ) was used. A seven fold increase in the bearing capacity was achieved for the optimum size of geocell mattress employed. Similarly, Mandal and Gupta [20] analyzed the performance of geocell, when placed in a sand layer underlying marine clay by performing laboratory tests and observed an improvement in the bearing capacity of the marine clay overlain by sand layer. From their study they concluded that the geocell with smaller opening size is found to be an appropriate reinforcement for paved roads with very less permissible settlements, whereas in the case of unpaved roads, large size geocells are observed to be effective. Table 2.1 summarizes the various studies performed by the researchers on the effectiveness of geocell mattress in improving the bearing capacity of the weak foundation beds.

**Table 2.1 Summary of studies performed on geocell mattress under static loading condition**

Study	Type of Facility	Geo-synthetics Used	Remarks
Bush et al. [10]	Embankment	Geocell	Enhanced bearing capacity.
Cowland and Wong [12]	Embankment on soft clay	Geocell	Enhanced bearing capacity
Mhaiskar and Mandal [21]	Soft Clay Subgrade	Geocell	improvement in the ultimate load and reduction in settlement
Krishnaswamy et al. [42]	Embankments constructed over soft clay bed	Geocell	Results depend on Stiffness of the geocell, pocket opening size, height of geocell, type of soil filled inside the geocell and the pattern used to form the geocells.
Dash et al. [15]	Laboratory tank	Geocell	Enhanced bearing capacity of strip footing on sandy ground
Saride et al. [43]	Laboratory tank	Geocell	Substantial increase in the bearing capacity and reduce settlement of the clay and sand subgrades under circular loading
Hegde et al. [23]	Laboratory tank	Geocell	The load carrying capacity of the geocell reinforced bed increased by 13 times for the aggregate in fill, 11 times for the sand infill and 10 times for the red soil infill.

## 2.3 Studies on geocell reinforcement under repeated load

The studies on the geo-synthetic reinforcement were started about five decades ago. Different reinforcement forms are being used for a long time viz. geo-textiles, geo-grids, geonets, geocomposites and geocells. Extensive literature is available on these materials as reinforcement (geo-grids and geocells) under static loading for pavement applications however, a very few studies are available on cyclic loading. Understanding of these mechanisms originated from static plate load tests, but later research have been focused on these mechanisms under cyclic loading.

It was noticed that the ultimate bearing capacity increases with increasing number of reinforcement layers under dynamic loading. Depth of placement of initial reinforcement and spacing between consecutive layers were kept constant ( $u/D = h/D = 0.33$ ) for all tests. Also, width of geo-synthetic reinforcement was maintained four times width of model footing. It was observed that increase in reinforcement layer (beyond  $N = 4$ ) does not enhance the improvement in bearing capacity. Dynamic load tests were conducted based on the optimum configuration obtained from static load test. Dynamic load was applied using a 16 rectangular shaped waveform and frequency of 1 Hz. Tests were conducted in a rigid steel tank measuring 760 mm from all sides and a square shaped rigid footing of side 76.2 mm (Halliday and potter [24]. Table 2.2 summarizes the various studies performed by the researchers on design of geo-synthetic reinforced pavements.

**Table 1.2 Summary of studies performed on design of geo-synthetic reinforced pavements**

Study	Type of Facility	Geo-synthetics Used	Remarks
Mengelt et al. [25]	large-size Triaxial cell	Geocell	Improved $M_r$ of the granular infill 1.4–3.2% by addition of geocell reinforcement.
Pokharel et al. [26]	Laboratory tank	Geocell	Single geocell reinforcement improved the stiffness of the reinforced sand by a factor of 1.5 compared to the unreinforced sand. Single geocell reinforcement increased the maximum load by two times from that of the unreinforced sand.
Moghaddas et al. [44]	Laboratory tank	Geocell	Reduce the plastic deformation under repeated loading compared to that under a similar static loading.
Yang et al. [45]	Accelerated Pavement Testing (APT)	Geocell	Reducing permanent deformations in unpaved roads

## 2.4 Studies on designing pavements with geo-synthetics

The design methods presently available for use of geo-grids in road base stabilization provide no or insufficient information about the required number of layers and the mechanical characteristics of geo-grids. Hence, a new design method has been developed which includes the design of geo-grids for road base stabilization, based on a four layer model: asphalt (binder and wearing course), base, subbase and subgrade. The base and/or subbase thickness has to be defined with one of the available methods such as AASHTO method [29], Giroud–Han method [6], Leng – Gabr method [30], etc. The proposed design methods can be used to calculate the tensile forces in the geo-grids generated by self-weight of the different layers; wheel load of heavy vehicles; membrane effect at the base (or subbase) subgrade interface. It is then possible to set the number and the mechanical characteristics of geo-grid layers required for absorbing the horizontal forces generated by these three mechanisms.

In recent years, many designers and leading geo-grid manufacturers favor the use of a parameter called layer coefficient ratio (LCR) to quantify the benefits of geo-grid reinforcement into pavement design. This approach is sensible and more technically correct. The LCR approach applies and limits the geo-synthetic benefit derived from trials to the specific layer improved by inclusion of reinforcement (granular base course layer) whereas the TBR approach applies to the whole pavement section. Therefore, extrapolation of TBRs derived from a limited set of trafficking trials to general pavement design may or may not be valid. On the other hand, the limited focus of the LCR is more robust, Table 2.3 summarizes the various studies performed by the researchers on pavement design methodologies adopting geo-synthetics. Figures 2.1 and 2.2 shows the variation of LCR with subgrade CBRs for different tensile strengths of geo-synthetic layers. It can be found that for planar geo-synthetic reinforcements, the LCR values are ranging from 1.2 to 1.9.

**Table 2.3 Summary of studies performed on design of geo-synthetic reinforced pavements**

Study	Geo-synthetics used	Remarks
Korulla et al. [30]	Geo-grid	Given the chart of LCR with change in CBR
Technical note [31]	Geo-grid	LCR ranges from 1 to 1.9 based upon CBR

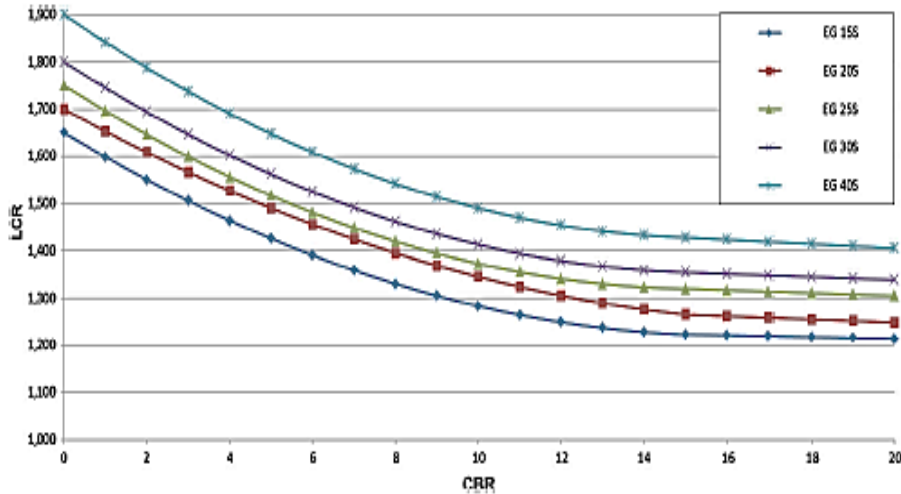


Figure 2.1 Variation of LCR with subgrade CBR [30]

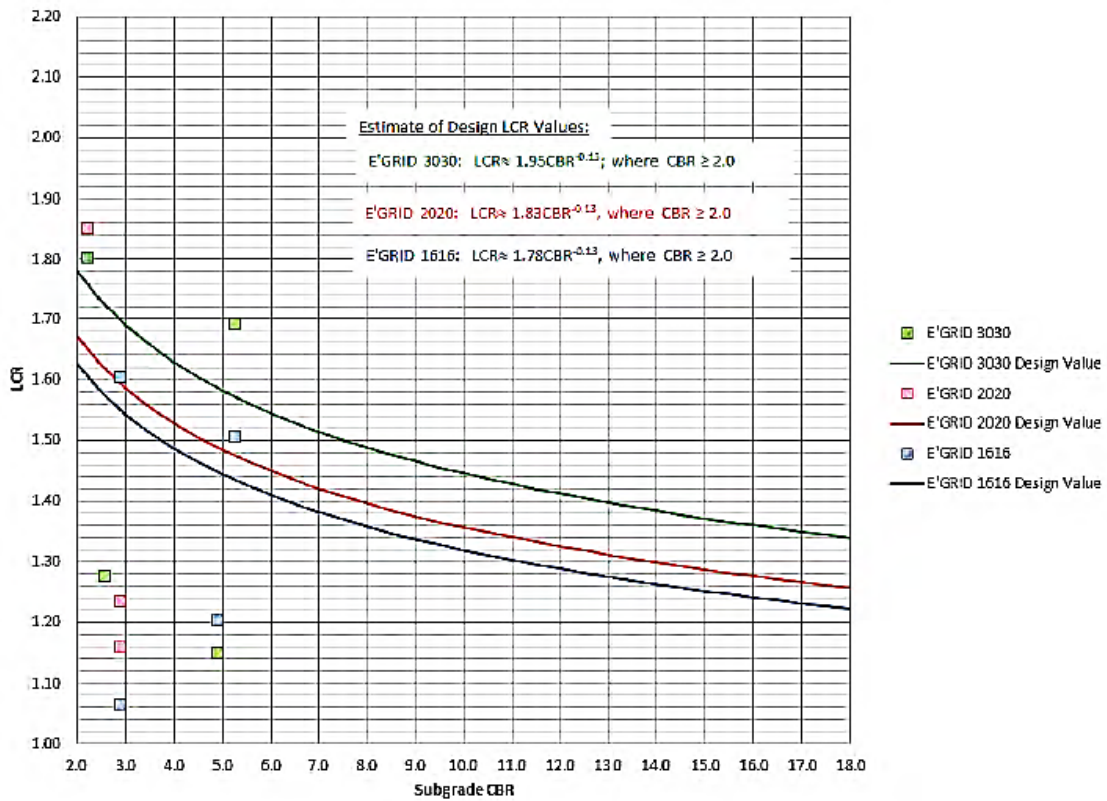


Figure 2.2 Estimate of LCR for Design based on Performance at 25 mm Permanent Deflection [31]

## 2.5 Summary

As discussed in the above sections, numerous large scale laboratory studies have been conducted on unreinforced and reinforced pavement bases. The performance in terms of Traffic Benefit Ratio (TBR) and the Layer Coefficient Ratio (LCR) have been listed in the Tables 2.1 & 2.3. From these

Tables, it can be noticed that the TBR& LCR have been significantly improved the performance of pavements. In India, limited studies are available on the geocell reinforced base layers on weak subgrade soils. In view of this, the current study focuses on the design of geocell reinforced pavement bases as per the IRC codal provisions and comparing it with the AASTHO specifications. Set of tests have been conducted on the unreinforced and geocell reinforced pavement sections in the laboratory and the test results have been discussed in the following chapters.



# Chapter 3

## Materials and Methods

### 3.1 Introduction

In this Chapter, the properties of different materials used and sample preparation techniques adopted in the present study are presented. The material properties are stated first and then the sample preparation procedures are elaborately discussed. The following materials are used in the study:

- Clayey sand to prepare a subgrade.
- Wet mix macadam (WMM) as a base course.
- Bituminous macadam as a surface layer.
- Geocell mattress as a base layer reinforcement.

The detailed characterization of each material is discussed below.

### 3.2 Characteristics of subgrade soil

The soil used for the study is natural lateritic clayey soil obtained from the permanent campus of Indian Institute of technology Hyderabad.

#### 3.2.1 Sieve analysis

A dry sieve analysis as per IS-2720 (Part4-1985) [32] was performed to determine the particle size distribution of the soil. Fig. 3.1 shows the particle size distribution of clayey soil, which consists of about 40% fines (i.e. particles smaller than  $75\mu$  sieve size). For further classification of the soil, Atterberg's limits tests were performed.

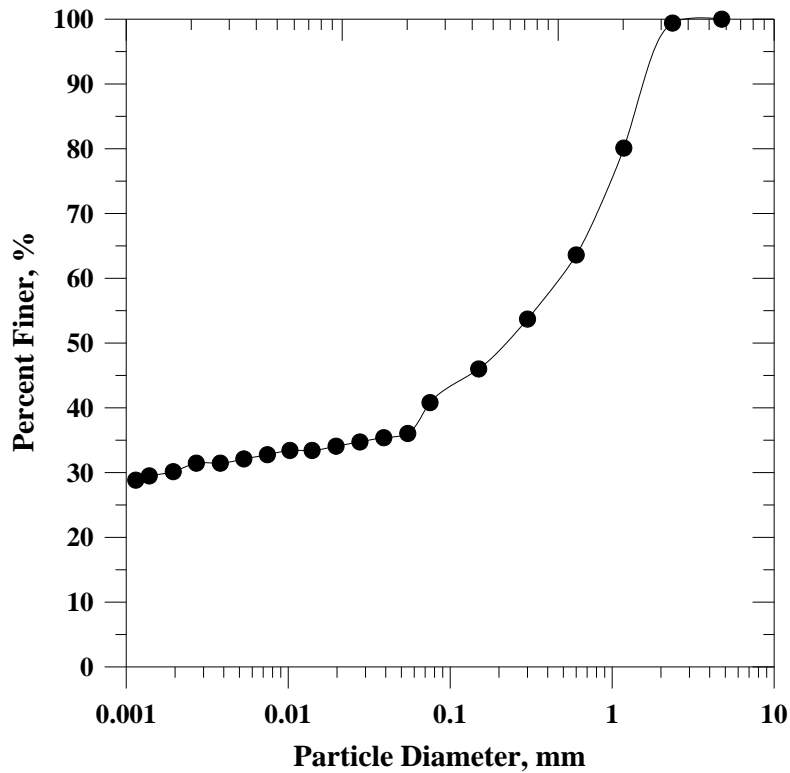


**Figure 3.1 Sieve analysis of the subgrade soil**

### **3.2.2 Atterberg’s limits**

Atterberg’s limits including liquid limit (LL) and plastic limit (PL) were conducted as per IS-2720 (Part4-1972) [33]. The images of apparatus used during this test can be seen in Fig.3.2a. Fig. 3.2b shows the flow curve of the soil. The liquid limit and plastic limit of the soil are found out to be 47% and 21% respectively. The Plasticity Index of the soil, which is the difference between LL and PL is found out to be 26%. As per the Indian standard soil classification system, the soil is found out to be well graded sand with clay (SC).

### **3.2.3 Specific gravity**

The specific gravity test is conducted as per IS-2720 (Part3-1980) [34] and the specific gravity is found out to be 2.65. This test is conducted by using density bottle method and the images of the test can be seen in Fig.3.3.



**Figure 3.2a Images of the LL and PL test**

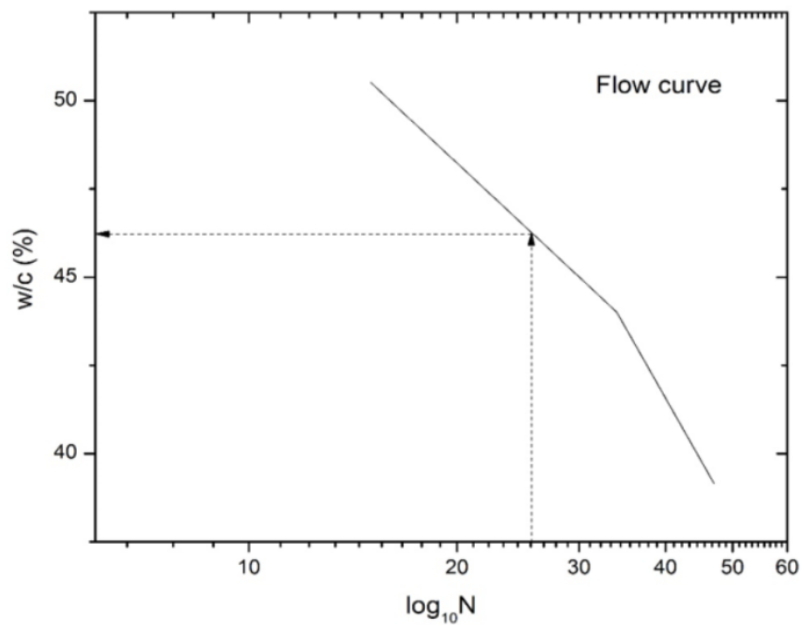


**Figure 3.2b Flow curve of clayey soil**



**Figure 3.3 Specific gravity test by density bottle method**

### **3.2.4 Compaction characteristics**

The Standard Proctor compaction test is a laboratory method of finding the optimum moisture content (OMC) and maximum dry unit weight (MDU) which is conducted as per IS-2720 (Part7-1980) [35]. According to the procedure, the soil is compacted in three layers in compaction mold of volume 948 cc and each layer is given 25 blows from a standard hammer of weight 2.6 kg and falling height of 310 mm.



**Figure 3.4 Mold and hammer used in standard proctor test**

The images of the apparatus used during the test are shown in Fig.3.4 and the relation between unit weight and moisture content is shown in Fig.3.5. From the graph, it is inferred that the optimum moisture content (OMC) is observed as 13.9% and maximum dry unit weight (MDU) as 18.25kN/m<sup>3</sup>.

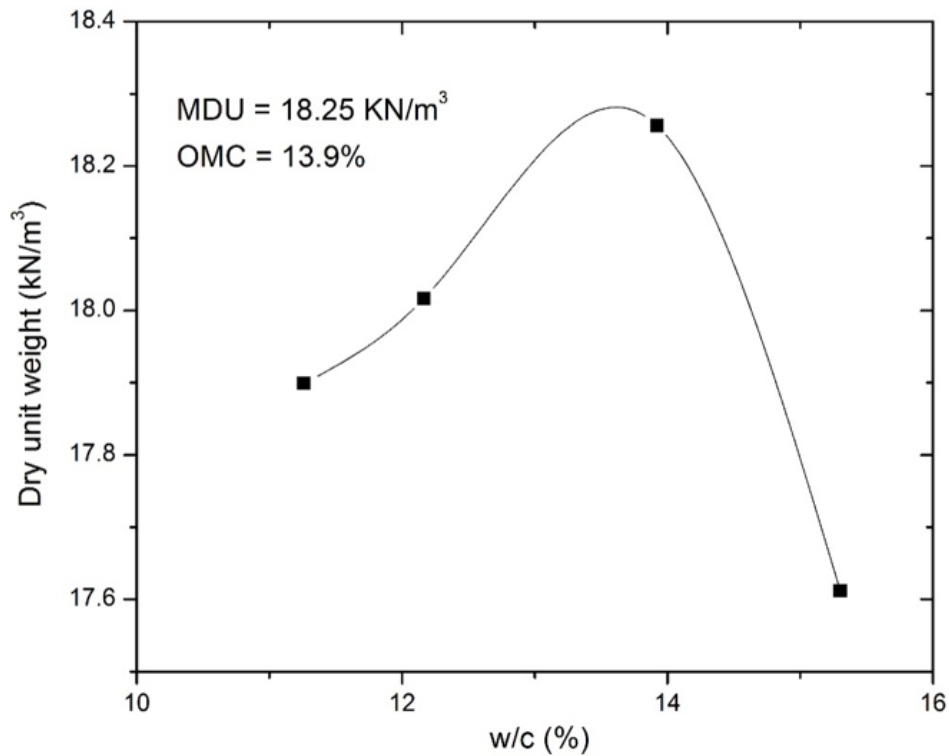


**Figure 3.5 Compaction characteristics of the subgrade soil**

### 3.2.5 California Bearing Ratio

The California bearing ratio (CBR) test is used to determine the bearing resistance of subgrade soils. According to Indian roads congress (IRC) guidelines, the flexible pavement design is dependent on this value. This test was conducted as per IS-2720 (Part16-1987) [36] on the subgrade clayey soil. The CBR setup is shown in Fig.3.6a.

The values of the CBR in soaked and unsoaked conditions are 4.9% and 7.8%, respectively. For further analysis and the design of pavement section, CBR of about 5% was considered. The results obtained are shown in Fig.3.6b.



Figure 3.6a CBR setup and post test specimen

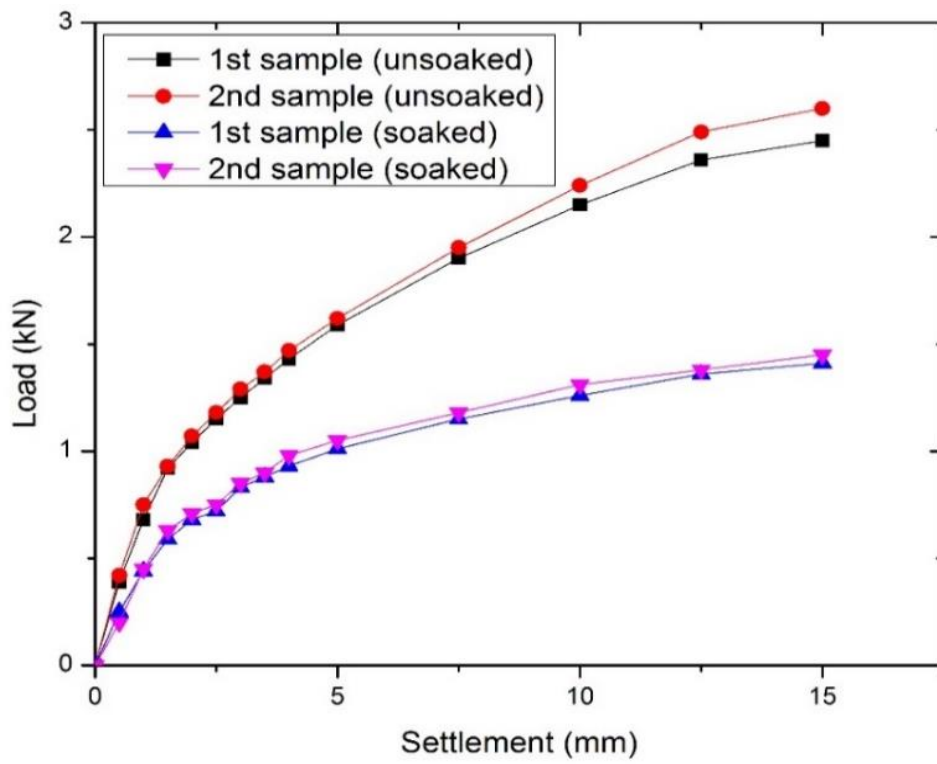


Figure 3.6b Load-settlement curve for CBR test

### 3.3 Characteristics of Wet Mix Macadam (WMM)

The wet mix macadam (WMM) is considered as per MORTH specification, 406.2.1.2. (Table 400-11) [37]. As per the MORTH, the aggregate shall conform to the grading given in Table 3.1 to be qualified as a base course material for the pavement. Aggregate material was obtained from a quarry near Kandi village to regrade and bin the material as per the MORTH's requirements.

**Table 3.1 Grading requirements of aggregates for Wet Mix Macadam**

IS Sieve	% by weight passing the IS
53	100
45	95-100
26.5	---
22.4	60-80
11.2	40-60
4.75	25-40
2.36	15-30
0.6	8-22
0.075	0-8

#### 3.3.1 Compaction characteristics

The Modified Proctor compaction test is a laboratory method of finding the optimum moisture content (OMC) and maximum dry unit weight (MDU) which is conducted as per IS-2720 (Part8-1980) [38]. According to the procedure, the material was compacted in 5 layers in compaction mold of volume 948 cc and each layer was given 25 blows from a standard hammer of weight 4.9 kg and falling height of 450 mm. Fig 3.7 shows the variation of unit weight with moisture content. From the graph, it is inferred that the OMC is about 6.5% and MDU as about 22.48 kN/m<sup>3</sup>.

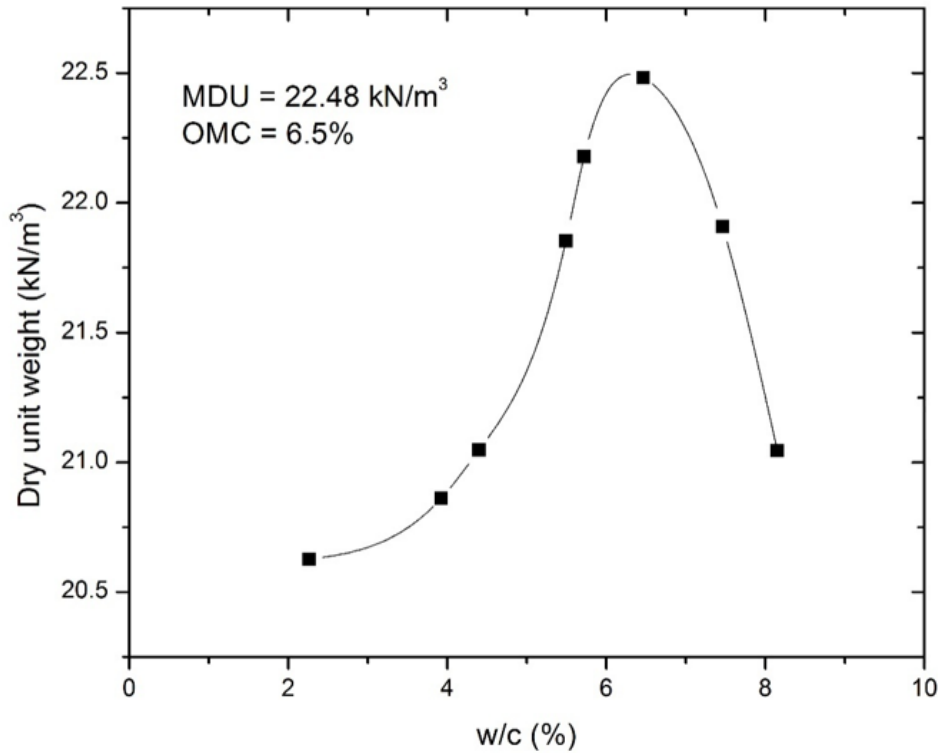


**Figure 3.7** Compaction characteristics of the Wet Mix Macadam layer

### 3.4 Characteristics of Geocell

Geocell is a three dimensional geo-synthetic material made up of high density polyethylene (HDPE) strips, ultrasonically welded at joints, expanded on site to form a honeycombed structure. Geocell binds the infill material and also provides lateral restraint to loading. Geocell mattress used in the current study is made up of a polymer of HDPE with a density ranging from 0.935 to 0.965 gm/cm<sup>3</sup> and a weld spacing of 356 mm. The height or depth of the cell is maintained at 200 mm with a minimum cell strength of 2100 N throughout the test series. A typical geocell mattress used in the given study can be seen in Fig. 3.8.





**Figure 3.8 Typical geocell used in the study**

### **3.5 Characteristics of bituminous course (BC) layer**

A visco-elastic bituminous concrete layer is laid as a surface course. Bitumen of penetration grade PG 60/70 was used with an optimum bitumen content is 5 to 6%. The composition of aggregates i.e. gradation of aggregates used in the bitumen concrete is presented in Table 3.2.

**Table 3.2 Grading requirements of aggregates for bitumen Layer**

IS sieve (mm)	Cumulative % by weight of total aggregate passing
26.5	100
19	79-100
13.2	59-79
9.5	52-72
4.75	35-55
2.36	28-44
1.18	20-34
0.6	15-27
0.3	10-20
0.15	5-13
0.075	2-8

## 3.6 Test methodology

### 3.6.1 Test setup

The subgrade soil was prepared and compacted at their required density and placement water content in a test tank measuring inner dimensions of  $1\text{ m} \times 1\text{ m} \times 1\text{ m}$  (length x width x height). On top of the subgrade soil a granular base layer i.e. WMM with and without geocell mattress were prepared. On the top of the base course layer a 50 mm thick layer of bituminous course was laid and compacted up to the required density. The test bed configuration and densities maintained will be discussed in the subsequent sections below. Once the final grade was prepared, a rigid thin steel plate of 150 mm diameter (D) and 15 mm thickness was concentrically placed to apply the appropriate static or repeated traffic loading. The size of the plate was chosen based on the previous experimental studies conducted in a similar testing by Edil et al. [39]. Loading was given by graphical user interfaced MTS MPT software with the help of hydraulic power unit (HPU), hydraulic service manifold (HSM) 34 and sophisticated double acting linear dynamic 100 kN capacity actuator which is attached to a 3.5 m high, 200 kN capacity reaction frame as shown in the below Fig. 3.9.

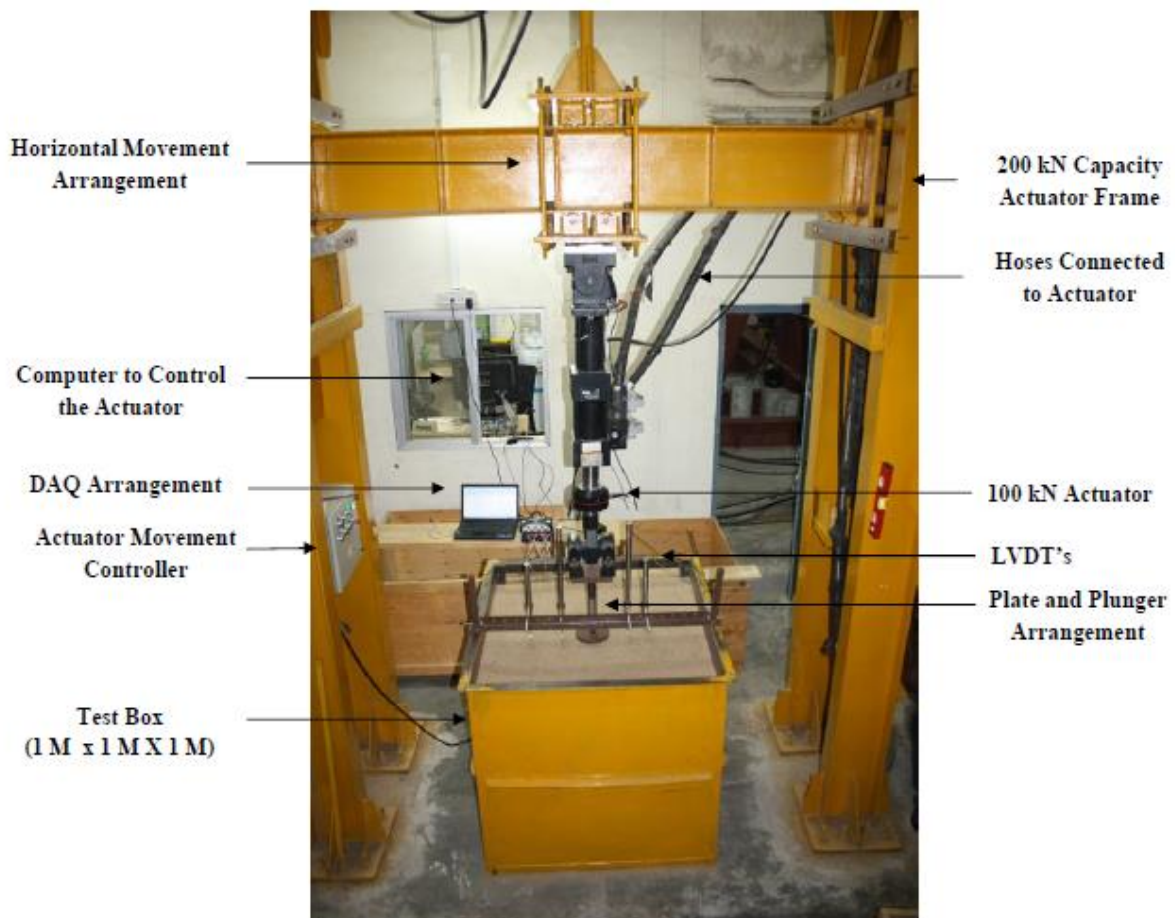


Figure 3.9 Large scale test setup

### 3.6.2 Preparation of test beds

Following are the stages adopted for the preparation of entire pavement section.

- Preparation of calibration charts.
- Preparation of subgrade.
- Preparation of base course layer.
- Preparation of bitumen course layer.

#### 3.6.2.1 Calibration charts

To determine the number of blows required to achieve the maximum dry unit weight in the test tank, initially, a calibration test tank of size  $0.6\text{m} \times 0.6\text{m} \times 0.6\text{m}$  was adopted. The pulverized soil was premixed with a required moisture content was filled in the tank with a 50 mm thick layer, which was then compacted with a hammer of weight 5kg falling from a free height 50cm on a plate size of  $200\text{mm} \times 200\text{mm}$ . The number of blows 3, 5, 7 and 9 were given in different trials, respectively, and measured the unit weights with the help of two core cutters of different sizes at every trial. A graph was then prepared to obtain the relation between the number of blows and the resultant unit weight. The calibration curve is shown in Fig. 3.10. From the graph it can be easily inferred that 8 blows are needed to achieve a required unit weight (MDU) of  $18.25\text{ kN/m}^3$ .

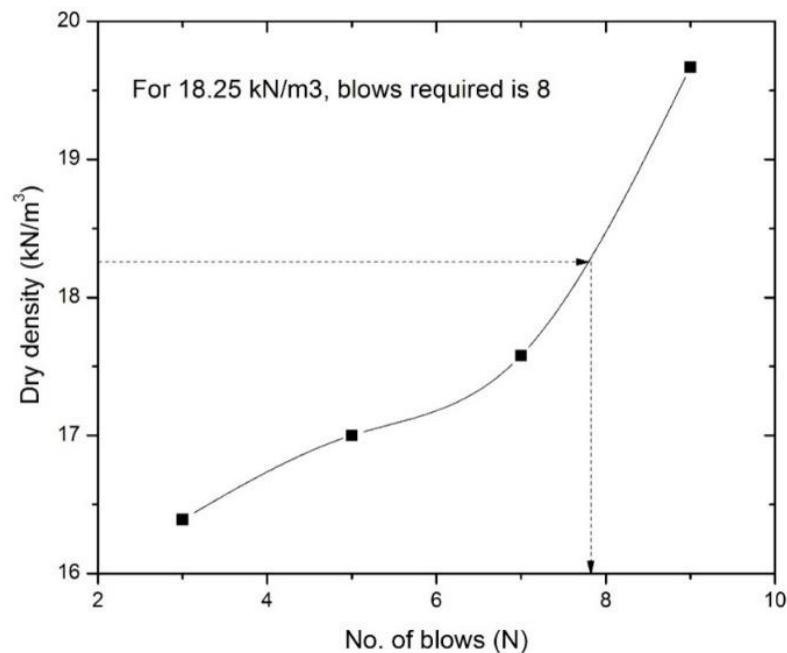


**Figure 3.10 Calibration curve for subgrade**

### **3.6.2.2 Subgrade preparation**

For the preparation of the subgrade, the soil was placed in the large test tank and compacted in 50 mm thick layers till the desired height was reached. For each layer the required amount of soil to produce a desired unit weight of 18.25 KN/m<sup>3</sup> was weighted and placed in the tank. The soil was then compacted using the 5kg drop hammer to a pre-calibrated number of blows (8 blows) to achieve the required unit weight. After each layer compaction, the level was checked.

### **3.6.2.3 Base course preparation**

To prepare the unreinforced test bed, the WMM material was placed in the test tank and compacted in 50 mm thick layers till the desired height was reached. For each layer the required amount of aggregate to produce a desired bulk unit weight 22.48 kN/m<sup>3</sup> was weighted out and placed in the test tank making use of a metal scoop. The granular base course was then gently leveled and compacted using a vibrator. After each layer compaction, the level was checked.

For the Geocell reinforced test bed, the compaction was done using a drop hammer of weight 5 kg, height of fall 50 cm with a plate size of 100 mm × 100 mm to allow a required compaction inside the individual geocell pockets. The compaction was done to achieve a layer height of 50 mm. The level was carefully checked after each layer compaction.

### **3.6.2.4 Preparation of Bitumen layer**

The aggregates were taken as per the grading specifications specified before, were then mixed with an optimum bitumen content of 5. A layer of tack coat was first sprayed on top of the base course layer and then the bitumen mix was placed on top of the base course layer. Then the layer was compacted with the help of a drop hammer. The material was compacted till 50 mm height of layer is achieved. The size of the surface layer is kept as 800 mm × 800 mm × 50 mm. Fig. 3.11 shows the complete overview of the test section.

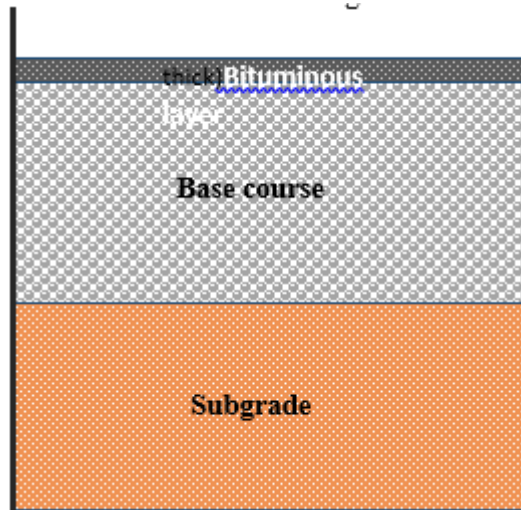


**Figure 3.11 A typical section shows the different layers**

Fig. 3.12 shows the staged preparation of test bed, the first image is of empty test tank of volume 1m<sup>3</sup>, in the second stage the soil is compacted for the subgrade bed, the third stage is the placing of pressure cells on top of the subgrade, the fourth stage is of placing the plate rod assembly along with geocell mattress, in the fifth stage the base layer is compacted till the required density achieved, in the next stage 4 plates are used which will be placed such that the dimensions of bituminous layer should be 80mm×80mm, the tack coat is then applied on the top of the base course layer so to get a proper bond between surface layer and base layer, after spraying of the tack coat the bituminous concrete material is poured and compacted properly to achieve the levelled surface.



**Figure 3.12 Various stages for the preparation of the test section**

### **3.6.3 Data acquisition system and instrumentation**



### 3.6.3.1 Data acquisition system (DAQ)

Data acquisition system (DAQ) from Hottinger Baldwin Messtechnik (HBM), Germany make is used to acquire the data from all the instrumentations used in the testing. There are two types of HBM's Quantum X data acquisition systems used namely MX 840 and MX 1615 which are seen in Fig. 3.13.



**Figure 3.13 DAQ Systems MX 840 and MX 1615**

The MX840A is an 8-channel universal amplifier which supports all current transducer technologies and MX1615 B which is the 16-channel universal amplifier used mostly in specific to strain gauges. The DAQ's are connected together using a fire wire cable which comes from the manufacturer.

Then the sensors are connected to the respective DAQ's after the connection arrangement is made. The sensors are then accessed by the laptop connected to the DAQ's by giving the information of the sensor like the excitation voltage, bridge resistance, sensitivities for the range of the sensors. Sensors are then checked and verified using the sensitivities given by the manufacturer. Otherwise, they are calibrated depending on the type of the sensor.

### 3.6.3.2 Multi-purpose test ware

Multi-Purpose Test ware (MPT) allows user to create complex test designs with discrete processes. Each process thus represents an individual test activity. A set of processes is grouped together in a closed loop to generate a have sine loading pattern.

The tests can be done into two ways viz. Force controlled method and Displacement controlled method. The tests done in the study were based on forced controlled method in which the configuration of devices provides a means of comparing a command signal (programmer output) to generate a signal with a feedback (transducer output) signal to generate a signal that controls a servo valve. The servo valve controls hydraulic flow of the actuator which moves the actuator piston rod. The actuator piston rod applies the force required to displace the component to be tested. Entire process is referred as "closed-loop control system" since, process of command, feedback, comparison

and servo valve is a function of control circuitry and occur without operator interaction. A typical MPT close-loop control program is shown in Fig. 3.14.

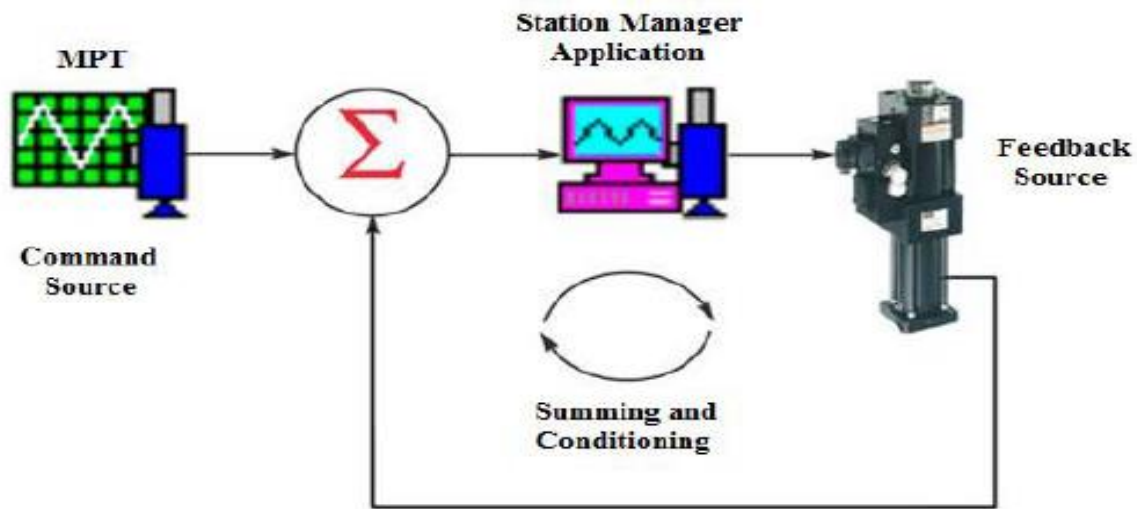


**Figure 3.14 Typical close-loop control program in MPT software**

### 3.6.4 Test procedure

The test procedures adopted for different types of tests are programmed using the multi-purpose test software of MTS for operating the hydraulic actuator. Upon filling the test tank up to the desired height, the fill surface was leveled and the loading plate was placed on a predetermined alignment such that the loads from the actuator would transfer concentrically to the loading plate. To ensure this, a recess was made into the loading plate at its center to accommodate a ball bearing through which vertical loads were applied to the loading plate. The loading plate was located carefully at the center of the hydraulic actuator mounted to the reaction frame of 3.5 m height to avoid eccentric loading. The actuator was then slowly moved close to the loading plate at a very slow rate such that the plate is in contact with the actuator. Each test according to the requirement was preloaded in the software and all the settings like the acquisition rate, loading rate and the loading pattern were set, then the test command was given to execute the test with the limits given in terms of displacement or force. Each type of tests was explained in the subsequent sections. In reinforced beds, the loading plate was allowed to settle till 25mm settlement of the plate. The load transferred to the loading plate and the settlements were measured through a pre-calibrated load cell and an in line LVDT placed along the actuator. The deformations (heave/settlement) of the pavement surface on either side of the plate were also measured using LVDT's placed at a distance of 1.0D and 1.5D from the centerline on either side of the loading plate. The settlement of the subgrade was also measure though a specially designed settlement plat and a cover placed at a distance of 1.0D from the edge of the plate. The readings from the LVDT's are recorded from the HBM make MX 840 data acquisition system (DAQ) along with the

testing. The pressure cells are installed on top of the subgrade at a distance 1D, 1.5D and 2D from the center line of loading plate and also at the center.

### 3.6.4.1 Static load tests

The static plate load tests were carried to estimate the ultimate strength for unreinforced and reinforced test sections. The test is carried out by applying a settlement or displacement rate of 0.5 mm/min. The response in terms of pressure and settlement is obtained to analyze the data further. Fig. 3.15a shows the loading pattern used in static loading test.

### 3.6.4.2 Repeated load tests

The repeated load test on the specimen is applied by carefully placing the plate at the center of the actuator against the reaction frame to avoid eccentric loading. Initially, the seating load was applied to a loading plate using a computer-controlled servo hydraulic actuator. The repeated load with a maximum load of 9.7 KN which is an equivalent pressure of 550 kPa (which is a typical tire pressure of a highway truck) and minimum load of 0.97 KN which is equivalent to 40 kPa is applied at a frequency of 1.0 Hz. A 10% of load (0.97 KN) was constantly applied on the plate to make the cycle a closed loop. This loading corresponds to the pressure transmitted on to the subgrade. Multi-Purpose Test Ware (MPT) software was set up to control and acquire the applied load data as well as the deformation data. The loading pattern adopted in this study can be seen in Fig. 3.15b.

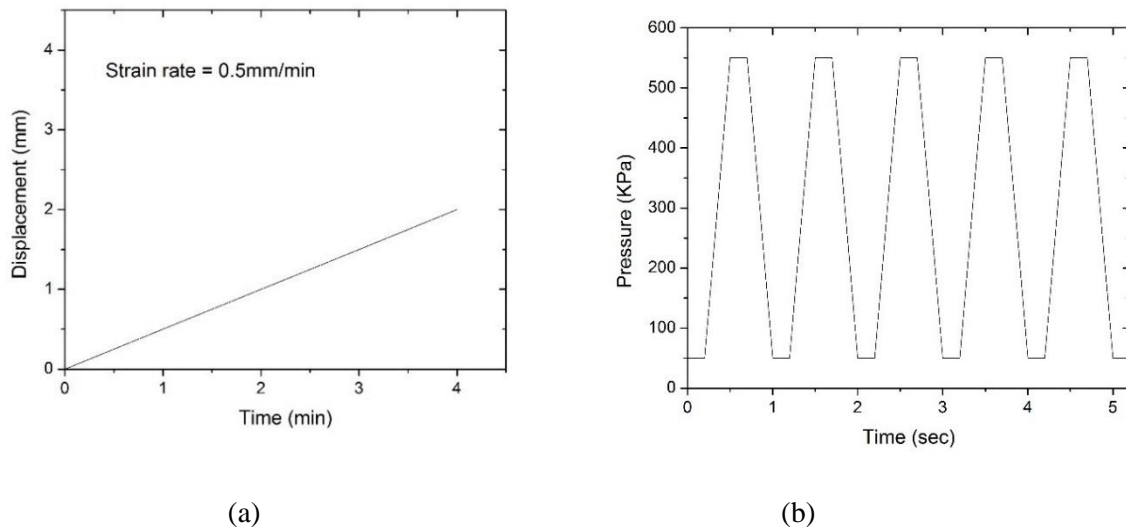


**Figure 3.15 Typical loading patterns (a) for static test (b) repeated load test**



### 3.7 Performance indicators

Several performance indicators are introduced to evaluate the efficacy of each reinforced test configuration over its counter unreinforced bed. These parameters are presented in the following sections.

#### 3.7.1 Cumulative permanent deformations

To analyze the data in terms of permanent deformations (or rutting), the total settlement accumulated from each cycle has been split up in to two components viz. elastic and plastic settlements as shown in Fig. 3.16. The plastic settlements (permanent deformations) are cumulatively added to obtain the cumulative permanent deformations (CPD).

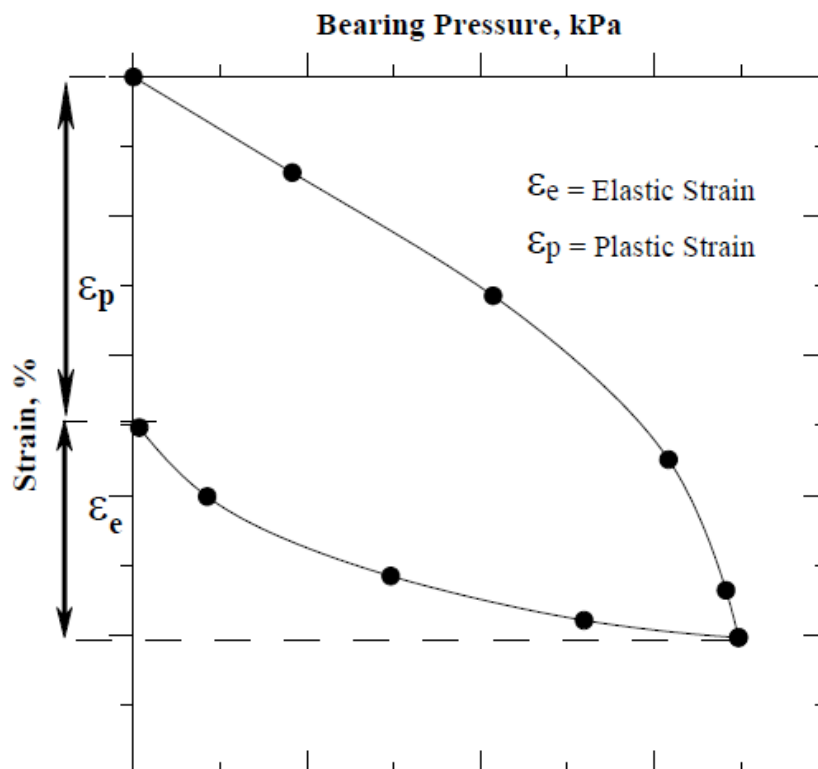


Figure 3.16 Elastic and plastic strains of a typical loading cycle

#### 3.7.2 Traffic benefit ratio

To quantify the benefits from the geo-synthetics especially in pavement applications, a non-dimensional term has been introduced and is expressed in terms of extension of life or by savings in base course thickness. Extension of life is defined in terms of a Traffic Benefit Ratio (TBR). TBR is defined as the ratio of the number of load repetitions necessary to reach a given rut depth for a test section containing reinforcement, divided by the number of repetitions necessary to reach the same rut

depth for an unreinforced section with the same section thickness and subgrade properties. The following is a mathematical expression for TBR evaluation.

$$TBR = \frac{N_r}{N_u} \quad (3.1)$$

where,  $N_r$  = No. of cycles required to reach given amount of rut depth

$N_u$  = No. of cycles required to reach same amount of rut depth

### 3.7.3 Rut depth reduction

To quantify the rutting behavior of geocell reinforcement, a parameter rut depth reduction (RDR), expressed in percentage, for different cases is introduced. RDR can be defined as the ratio of difference between cumulative permanent deformations of the unreinforced bed ( $CPD_{unrein}$ ) and geocell reinforced bed ( $CPD_{reinf}$ ) to that of the unreinforced bed for a particular number of loading cycle. Hence, RDR for an nth load cycle can be expressed as:

$$(RDR)_N = \left(1 - \frac{CPD_{reinf}}{CPD_{unrein}}\right) \times 100 \quad (3.2)$$

### 3.7.4 Equivalent modulus improvement factor

Equivalent modulus improvement factor (EMIF) is a ratio of total elastic modulus of reinforced test section ( $E_r$ ) to the total elastic modulus of the unreinforced test section ( $E_u$ ) with the same test configuration. The equivalent modulus improvement factor is introduced to quantify the effect of geocell reinforcement in the pavement test section. This parameter is very important in analyzing the pavement sections and their design.

$$EMIF = \frac{E_{reinf}}{E_{unrein}} \quad (3.3)$$

### 3.7.5 Rut benefit ratio

To quantify the rutting behavior of geocell reinforcement at the subgrade level, a parameter known as rut benefit ratio (RBR), expressed in percentage, for different cases is introduced. RBR can be defined as the ratio of difference between cumulative permanent deformations of the unreinforced bed ( $CPD_{unrein}$ ) and geocell reinforced bed ( $CPD_{reinf}$ ) to that of the unreinforced bed for a particular number of loading cycle. However, CPDs are precisely measured on the subgrade surface. Hence, RBR for an nth load cycle can be expressed as:

$$(RBR)_N = \left(1 - \frac{CPD_{\text{reinf}}}{CPD_{\text{unreinf}}}\right) \times 100 \quad (3.4)$$

### 3.7.6 Layer coefficient ratio

Layer coefficient ratio (LCR) is defined as the ratio of layer coefficients of reinforced to that of unreinforced layer. It is a measure of improved structural capacity of the reinforced pavement layer. While reinforcing base layers, it is calculated as:

$$LCR = \frac{0.249 \log_{10}(EMIF \cdot M_{r2}/0.0069) - 0.977}{0.249 \log_{10}(M_{r2}/0.0069) - 0.977} \quad (3.5)$$

where,  $M_{r2}$  = Resilient modulus of base course layer

## 3.8 Summary

Overall, a detailed experimental program has been evaluated and discussed all the methods to be adopted and materials to be used in this chapter to design a real pavement section for a known CBR value of the subgrade.

# Chapter 4

## Results and Discussion

### 4.1 Introduction

In this chapter, the pavement test sections were designed according to the IRC37-2012 [40] guidelines based on the material properties (CBR=5%). The design pavement test sections with and without geocell reinforced base layers were tested by applying a static load at a uniform displacement rate of 0.5 mm/min. Further, based on the equivalent modulus improvement factor obtained from the pressure-settlement curves, the geocell reinforced test sections were re-designed with a reduced base thickness. As mentioned in the previous chapter, the proposed methodology is followed to carry out the large scale testing program. The static and repeated load tests performed on these test sections are discussed in detail along with the design approach involved in the following sections.

### 4.2 Design approach

The flexible pavements are designed as a layered system in which the wheel loads are transferred to the lower layers by distributing the loads to a wider area. The stresses and strains at critical locations are computed using linear elastic models. The pavements should be designed such that they should perform efficiently throughout their design life. The failure of flexible pavements is generally due to fatigue cracking and the formation of ruts, which can be visualized on the pavement surface.

1. Vertical compressive strain at the top of the sub-grade which can cause sub-grade deformation resulting in permanent deformation at the pavement surface.
2. Horizontal tensile strain or stress at the bottom of the bituminous layer which can cause fracture of the bituminous layer.

The design methodology (as per IRC 37-2012) [40] adopted in the current study is discussed in the following steps.

Step 1. Finding the allowable fatigue and rutting strains at critical locations.

Fatigue strain is the horizontal tensile strain ( $\epsilon_t$ ) at the bottom of the bituminous bound layer, which is an indicator for fatigue cracking in the bituminous layer. Rutting strain is the vertical strain on top of the subgrade ( $\epsilon_v$ ), which is considered to be causative factor for permanent deformation in subgrade (Fig. 4.1). The allowable fatigue and rutting strains are computed from the following models specified in IRC37-2012 [40].

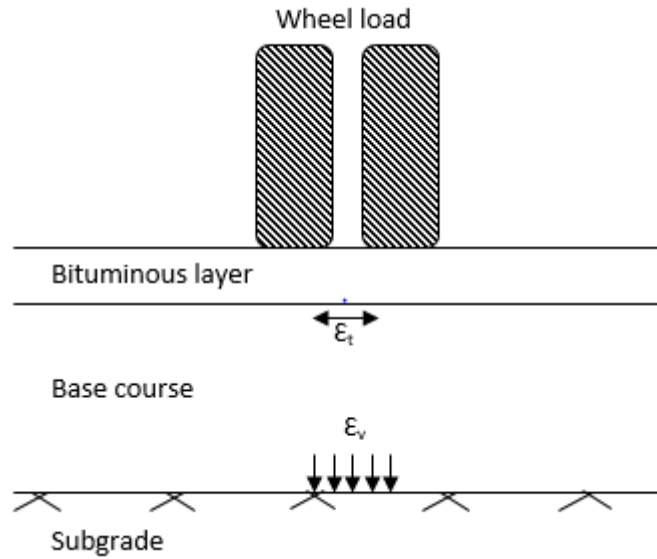


**Figure 4.1 Locations of critical strains**

Fatigue equation for 90% reliability is given as:

$$N_f = 0.711 \times 10^{-4} \times \left( \frac{1}{\epsilon_t} \right)^{3.89} \times \left( \frac{1}{M_R} \right)^{0.854} \quad (4.1)$$

Where,  $N_f$  = fatigue life in number of cycles

$\epsilon_t$  = Maximum tensile strain at the bottom of bituminous layer

$M_R$  = Resilient modulus of bituminous layer

Rutting equation for 90% reliability is given as:

$$N_f = 1.41 \times 10^{-8} \times \left( \frac{1}{\epsilon_v} \right)^{4.5337} \quad (4.2)$$

Where,  $N$  = Number of cumulative standard axles

$\epsilon_v$  = Vertical strain in subgrade

Step 2. Selecting an appropriate thickness of pavement layers from the design charts (CBR Plates)

Thickness of the pavement layers are computed from the design catalogues given in IRC for relevant traffic and subgrade conditions.

### Step 3. Finding the fatigue and rutting strains using IITPAVE

As discussed earlier, IITPAVE, a computer program developed by IIT Kharagpur is used to find out the strains at the critical locations as shown in Fig. 4.1. Incorporating the above trial thickness in the IITPAVE software, fatigue and rutting strains for the selected pavement section are computed and are verified against the allowable strains.

### Step 4. Arriving at the final thickness

For a safe and efficient pavement system, the fatigue and rutting strains (obtained in step 3) should be less than the limiting fatigue and rutting strains (obtained in step 1). If the strains obtained are less than the limiting strains, the selected pavement section thicknesses can be adopted.

Based on the above design procedure, for a subgrade soil CBR of 5% and a traffic equivalent to 2 msa, the CBR plate shown in Fig. 4.2 is referred to obtain the design pavement section thicknesses. The pavement thickness corresponding to the subgrade condition and the expected traffic flow are provided in the design catalogues of IRC 37:2012 [40].

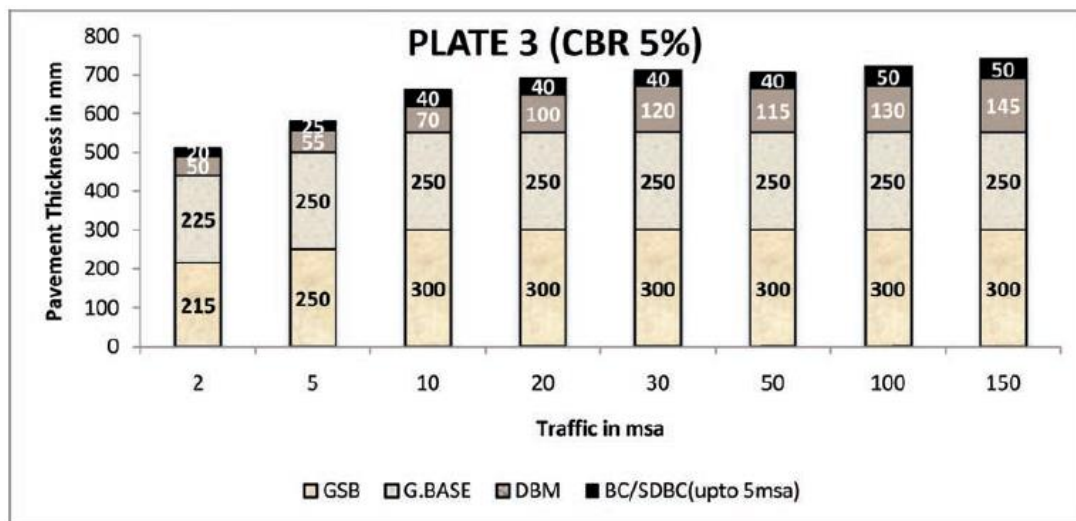


Figure 4.2 Typical pavement design chart for subgrade CBR of 5% (IRC 37:2012)

From Fig. 4.2, as per the subgrade and traffic conditions mentioned above, a pavement test section with a total thickness of 510mm was obtained. The pavement section consists of a 215mm granular sub-base layer, 225mm granular base layer, 50mm thick dense bituminous macadam and a 20mm thick bituminous concrete layer. However, as per the design steps explained above, the total thickness of the pavement section is found to be 490mm comprising of 440mm of granular base and sub-base layers and a 50mm thick bituminous concrete layer.

#### 4.2.1 Verifying the results of IRC using AASHTO (1993)

The thicknesses and the properties of the pavement layers provided in Table 4.1 were incorporated in the AASHTO (1993) [29] design equations and it was witnessed that the number of repetitions were reduced to 0.66msa in place of 2 msa, obtained from IRC charts. This observation suggest that, either the IRC is under predicting the pavement layer thicknesses or over predicting the expected traffic flow.

**Table 4.1 Results from AASHTO method [29]**

Input parameters	Results
$E_{AC} = 435113 \text{ psi}$	$SN_u = 3.06$ $W_{18} = 0.66 \text{ msa}$
$E_B = 22336 \text{ psi}$	
$M_R = 7252 \text{ psi}$	
$Z_R = -1.282$	
$S_o = 0.45$	
$\Delta PSI = 2.3$	

Table 2 provides the comparison of results obtained from both the IRC and AASHTO pavement design methodologies and it can be inferred that the correlations used to calculate the  $M_R$  of base layer in IRC method is inappropriate, because the IRC method considers subgrade CBR to calculate the base layer  $M_R$ .

**Table 4.2 Comparison of the results**

$M_R = 154 \text{ MPa}$		$M_R = 200 \text{ MPa}$	
IRC	AASHTO		
Traffic = 2 msa	$S_{NU} = 3.06$	Traffic = 2 msa	Traffic = 2 msa
CBR = 5%	$D_2 = 440 \text{ mm}$	$S_{NU} = 3.65$	$S_{NU} = 3.65$
$D_2 = 440 \text{ mm}$	Traffic = 0.67 msa	$D_2 = 553 \text{ mm}$	$D_2 = 439 \text{ mm}$

Table 4.3 provides the comparison of tensile and compressive strains obtained from the IITPAVE software with the limiting strains obtained from the equations as per IRC 37 [40]. The IRC results are verified using IIT PAVE software and AASHTO results are verified using KENPAVE software.

**Table 4.3 Comparison of the strains obtained and limiting strains**

Thickness of base layer	For $M_R = 154\text{MPa}$		For $M_R = 200\text{MPa}$
	Limiting strains	Strain values from Software	Strain values from Software
440 mm	$\varepsilon_t = 0.47544 \times 10^{-3}$	$\varepsilon_t = 0.4210 \times 10^{-3}$	$\varepsilon_t = 0.3332 \times 10^{-3}$
		$\varepsilon_v = 0.8237 \times 10^{-3}$	$\varepsilon_v = 0.7370 \times 10^{-3}$
553 mm	$\varepsilon_v = 0.96 \times 10^{-3}$	$\varepsilon_t = 0.419 \times 10^{-3}$	$\varepsilon_t = 0.33 \times 10^{-3}$
		$\varepsilon_v = 0.563 \times 10^{-3}$	$\varepsilon_v = 0.5017 \times 10^{-3}$

#### 4.2.2 AASHTO design method through TBR approach (reinforced pavement section) [41]

Step1: The structural number (SN) is calculated for the unreinforced test section by using the following equation.

$$SN_u = a_1 D_1 + a_2 D_2 m_2 \quad (4.3)$$

Where,  $SN_u$  = structural number for unreinforced case

$a_1$  = Layer coefficient for surface layer and is calculated using the following equation

$$a_1 = 0.171 (\ln (E_{AC}) - 1.784) \quad (4.4)$$

$d_1$  = thickness of asphalt layer (mm)

$a_2$  = layer coefficient for granular base layer and is calculated the below equation

$$a_2 = 0.249 (\log_{10} (E_{BC})) - 0.977 \quad (4.5)$$

$d_2$  = thickness of base course layer (mm)

$m_2$  = drainage coefficient for base layer

$E_{AC}$  = modulus of elasticity of asphalt layer

$E_{BC}$  = modulus of elasticity of base layer

Step 2: By using the TBR value calculated from the repeated loading test, the designed traffic (in msa) is multiplied with TBR to get the value of modified traffic value (in msa) for the reinforced pavement section.



Step 3: The structural number (SN) is calculated for reinforced test section by using the equation written below. The value of traffic substitute in the following equation should be the modified one.

$$\text{Log}_{10}(W_{18}) = Z_R S_o + 9.36 \log_{10} (\text{SN}_R + 1) - 0.20 + \frac{\log_{10} \left[ \frac{\Delta \text{PSI}}{4.2 - 1.5} \right]}{0.40 + \frac{1.094}{(\text{SN}_R + 1)^{5.19}}} + 2.32 \log_{10} M_r - 8.07 \quad (4.6)$$

Where,  $W_{18}$  = predicted number of 18-kip (80-kN) ESALs

$Z_R$  = standard normal deviate (dimensionless)

$S_o$  = combined standard error of the traffic prediction and performance prediction (dimensionless), 0.45 commonly used

$\Delta \text{PSI}$  = difference between the initial present serviceability index ( $P_0$ ) and the design terminal pavement serviceability index ( $P_t$ )

$\text{SN}$  = structural number of reinforced pavement layer

$M_r$  = resilient modulus of roadbed (MPa)

Step 4: The  $\text{SN}_R$  is then subtracted with  $\text{SN}_u$  to get the value which is virtually inducing due to the inclusion of the geocell in the basal layer.

Step 5: Keeping the  $\text{SN}_u$  constant and by changing the values of  $d_2$  in eq. (4.3) the structural number is then find out which is further added with the value induced due to reinforcement in the pavement section. If the value of  $\text{SN}_u$  matches with equivalent structural number calculated as discussed above, then the corresponding  $d_2$  is the revised thickness of the base course layer in reinforced case which is equivalent to the earlier thickness of the unreinforced section.

**Table 4.4 Reinforced pavement design [41]**

Input parameters	Results
$E_{AC} = 435113 \text{ psi}$	$SN_u = 3.65$ $TBR = 3.5$ $(D_2)_U = 440 \text{ mm}$ $(D_2)_R = 271 \text{ mm}$
$E_{Br} = 37710 \text{ psi}$	
$M_I = 7252 \text{ psi}$	
$Z_R = -1.282$	
$S_o = 0.45$	
$\Delta PSI = 2.3$	
$TBR = 3.5$	
$W_{18} = 2 \text{ msa}$	

#### 4.2.3 AASHTO design through LCR approach (reinforced pavement section)

$$LCR = \frac{0.249 \log_{10}(EMIF \cdot M_{R2}/0.0069) - 0.977}{0.249 \log_{10}(M_{R2}/0.0069) - 0.977} \quad (4.7)$$

$$(D_2)_R = \frac{SN - a_1 D_1}{LCR a_2 m_2} \quad (4.8)$$

Where,  $D_{2(R)}$  = Thickness of base layer in mm

Further, as per the test section designed, a subgrade of 410mm was compacted in 8 layers each of around 50mm thick and the base course layer was compacted in 9 layers each of about 50mm thick. A bituminous concrete of 50mm thickness was then compacted after the application of tack coat on the dry base course.

The static load tests were performed on the unreinforced and geocell reinforced test sections with a base course thickness of 440 mm to understand the influence of geocell reinforcement in improving the modulus of the base course layer, which in turn improves the performance of entire pavement system. The equivalent modulus improvement factor (EMIF) is estimated with the help of these static load tests performed and the detailed procedure is explained in the following section.

### 4.3 Equivalent modulus improvement factor

To determine the equivalent modulus improvement factor (EMIF), static load tests were performed on the unreinforced and the geocell reinforced pavement test sections obtained as per the design approach adopted. The static load test results are obtained in the form of pressure-settlement curves for the unreinforced and geocell reinforced test sections separately as presented in Fig. 4.3. From Fig. 4.3, it can be observed that the bearing pressure in the reinforced test section is as high as 3200kPa at 25 mm settlement. Whereas, the bearing pressure in the case of unreinforced test section at the same settlement (25 mm) is observed to be 2130 kPa. This observation suggests the fact that the presence of geocell reinforcement has improved the bearing pressure by almost 1.5 times the control section at 25mm settlement.

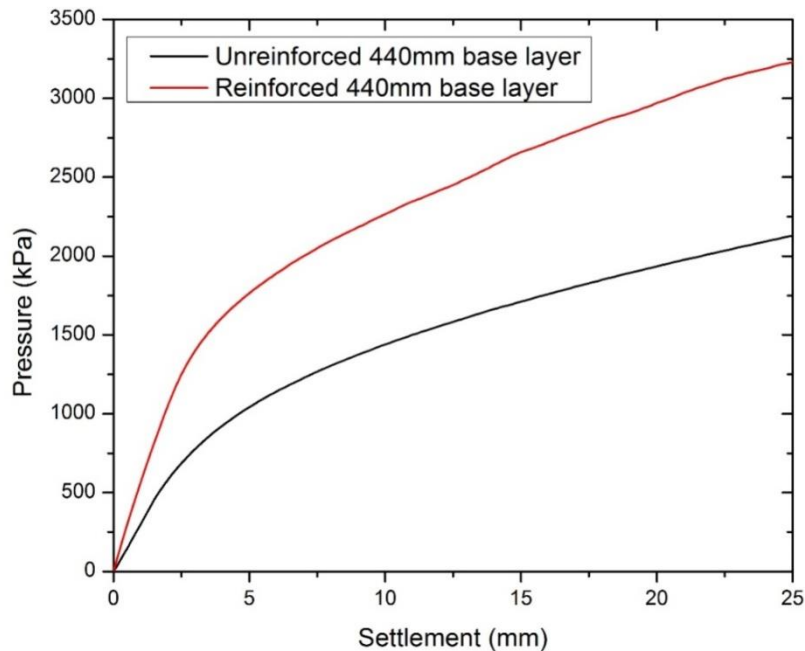


**Figure 4.3 Pressure-settlement curve for 440mm thick base geocell reinforced and unreinforced test sections**

The elastic modulus is calculated from the linear or elastic region of the stress-strain plots obtained for both the reinforced and unreinforced test sections. The elastic modulus obtained in both the cases are the equivalent module of the entire pavement test section, as the stress-strain curves are plotted for the static load test results obtained from the unreinforced and reinforced test sections. The EMIF can be defined as the ratio of elastic modulus of reinforced section to the elastic modulus of the unreinforced section. An EMIF of about 2.24 is achieved in the geocell reinforced test sections against

the control test section. Hence, it can be inferred that the presence of geocell reinforcement has improved the stiffness of the base course layer.

Further, in geocell reinforced base layer, to maintain the same stiffness as that of unreinforced test sections, the thickness of geocell reinforced base layers can be reduced in such a way that an EMIF greater than 1 should be maintained. Hence, the base course thickness of reinforced test section was reduced from 440 mm to 250 mm and static load tests were performed on the test sections with reduced thickness. The tests were performed on the sections with reduced thickness to verify whether the EMIF value obtained is greater than 1. An EMIF of 1.3 was obtained for the geocell reinforced reduced base course thickness.

The experimental program is briefly divided into two stages as shown in Table 4.5

**Table 4.5 Test summary**

Stage	Test program	Configuration
1	Static load test	Unreinforced test section having 440 mm thick base course Reinforced test section having 440/250 mm thick base course
2	Repeated load test	Unreinforced test section having 440 mm thick base course Reinforced test section having 250 mm thick base course

#### 4.4 Static load test results

During the first stage, the static load tests were performed on the unreinforced test section having a 440mm thick base course (Fig. 4.4) and a geocell reinforced test section having a 250mm thick base course (Fig. 4.5) to understand the influence of geocell reinforcement in improving the base layer stiffness and also to study the performance of geocell under static load conditions. The loads were applied on the test sections at a constant settlement rate of 0.5mm/min until a settlement of about 25mm is reached and the corresponding load applied are noted. The pressure-settlement curves obtained for the test sections shown in Figs. 4.4 and 4.5 are as presented in Fig. 4.6. From Fig. 4.6, it can be observed that for the same level of settlement the reinforced section is bearing more pressure than the unreinforced one. For instance at 5mm settlement, the bearing pressure in unreinforced case is 900kPa, whereas it is 1200kPa in reinforced case. Similarly at 25mm settlement, the bearing pressure in unreinforced section is 2130kPa as compared to 2330kPa in reinforced section. So, at

25mm settlement a percentage increase of about 9.39% in bearing pressure is observed in reinforced case.

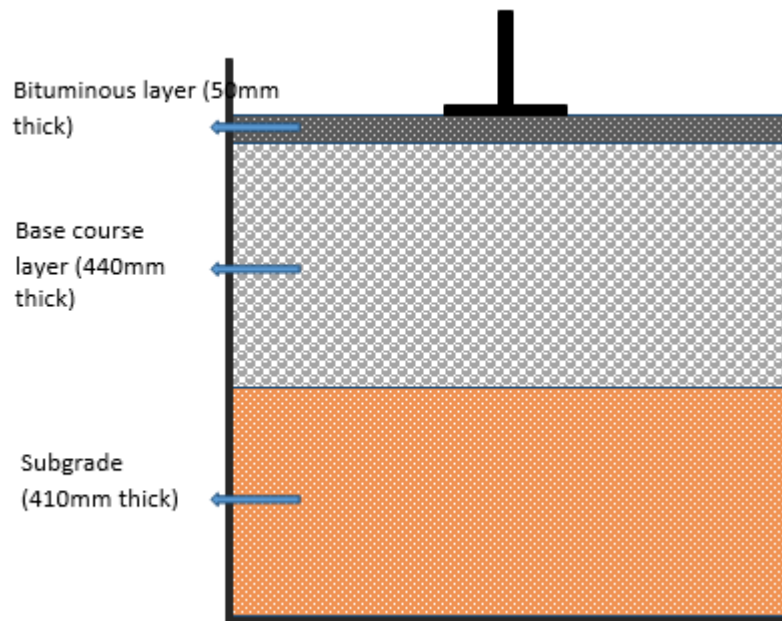


**Figure 4.4 Unreinforced test section used in the study**

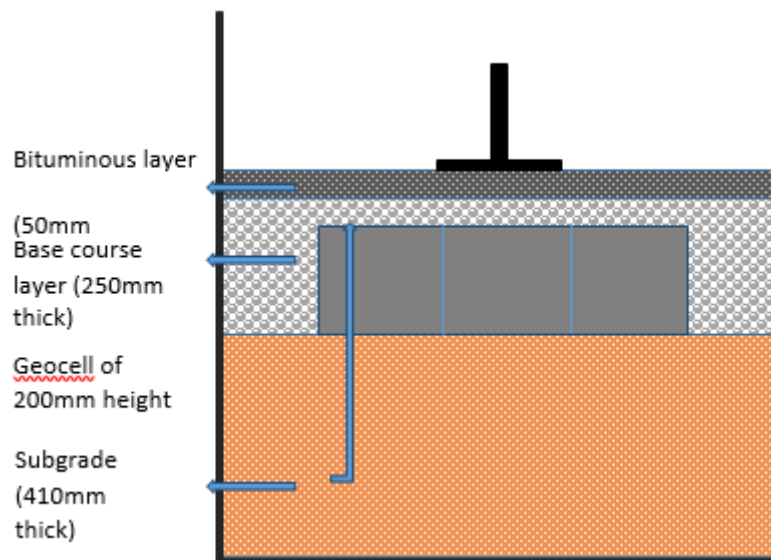


**Figure 4.5 Reinforced test section used in the study**

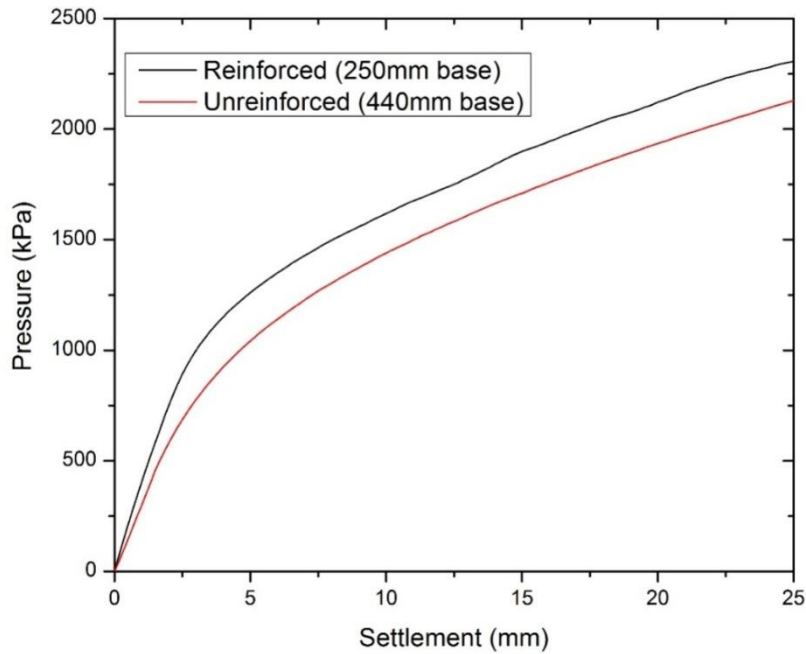


**Figure 4.6 Pressure-settlement curve for 440mm thick unreinforced and 250mm thick base geocell reinforced test sections**

The surface deformations and the deformation profile for both unreinforced and geocell reinforced test sections were obtained with the help of the displacement sensors located in the actuator and also the LVDTs placed at a distance of 1D and 1.5D on either sides from the centerline of loading point as explained in section 3.6.4. Figure 4.7 presents the deformation profile for the unreinforced test section in the form of deflection basins. The term deflection basin can be defined as the area of pavement deflection under and near the loading region. It can be observed from Fig. 4.7 that with the increase in the pressure applied, the deflection basin gets deeper i.e. the settlement is high. However, the settlement is mainly observed below the loading region and the settlements are observed to be very less to negligible on either sides of the loading region. For Instance, at an applied pressure of 1500 kPa, the settlement of the loading plate is as high as 11mm whereas, the settlements on either sides of loading plate are observed to be 2 mm and 1 mm at a distance of 1D and 1.5D from centerline respectively.

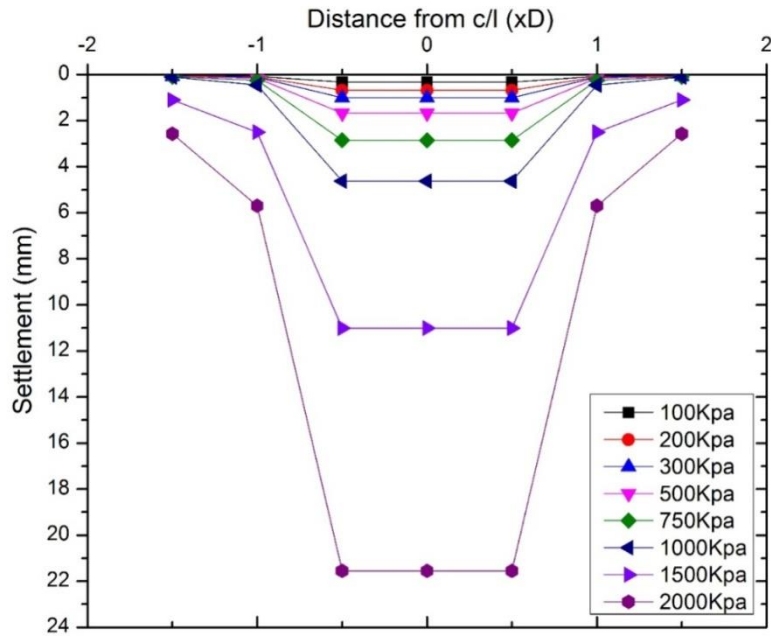


**Figure 4.7 Surface deformation profile of unreinforced test section**

Similarly, Fig. 4.8 presents the deformation profile of the geocell reinforced test section in the form of deflection basins. It can be observed from Figs 4.7 and 4.8 that for the same amount of pressure applied, the geocell reinforced section has restricted the settlement reasonably. It can also be observed from Fig. 4.7 and Fig. 4.8 that, the settlements in both the test sections are almost similar up to a pressure of 300kPa is applied. Further, with the increase in applied pressure, the settlements in the unreinforced sections has increased drastically compared to the geocell reinforced section. From this observation, it can be inferred that the presence of geocell reinforcement in the base layer has improved the stiffness of the base layer and in turn has reduced the surface settlements of the test section.

The test sections were also instrumented with the pressure cells located at the subgrade level exactly below the loading region and at a relative distance of 1D, 1.5D and 2D from the centerline of the loading region as explained in the section 3.6.4. The pressure acting on the subgrade due to the various intensities of load applied on the surface of the test sections can be determined with the help of this instrumentation arrangement and both the unreinforced and geocell reinforced test sections were instrumented to understand the pressure distribution patterns in the pavement system. Figure 4.9 presents the pressure distribution patterns at the subgrade levels for various intensities of pressure applied on an unreinforced test section. It can be observed that, with the increase in the applied pressure, there is an increase in the pressure acting on the subgrade. The pressure distribution curve

gets sharper with an increase in applied pressure i.e. the pressure recorded exactly below the loading region is high. However, the pressure acting at a distance of 1.5D and 2D are relatively less.

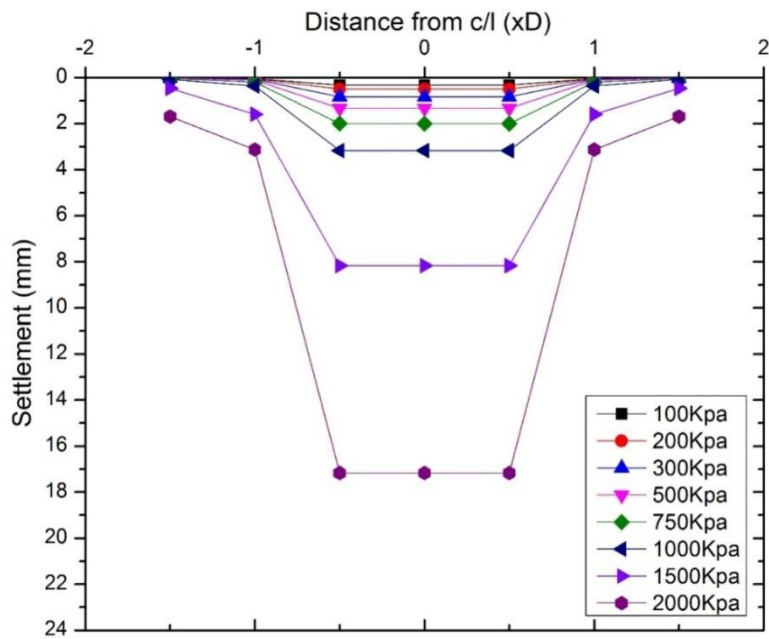


Figure 4.8 Surface deformation profile of reinforced test section (250mm base)

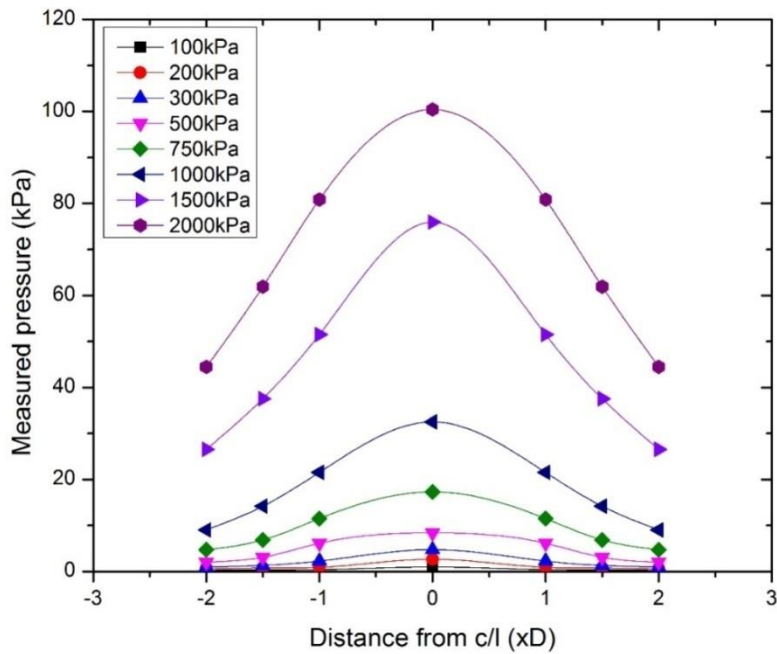
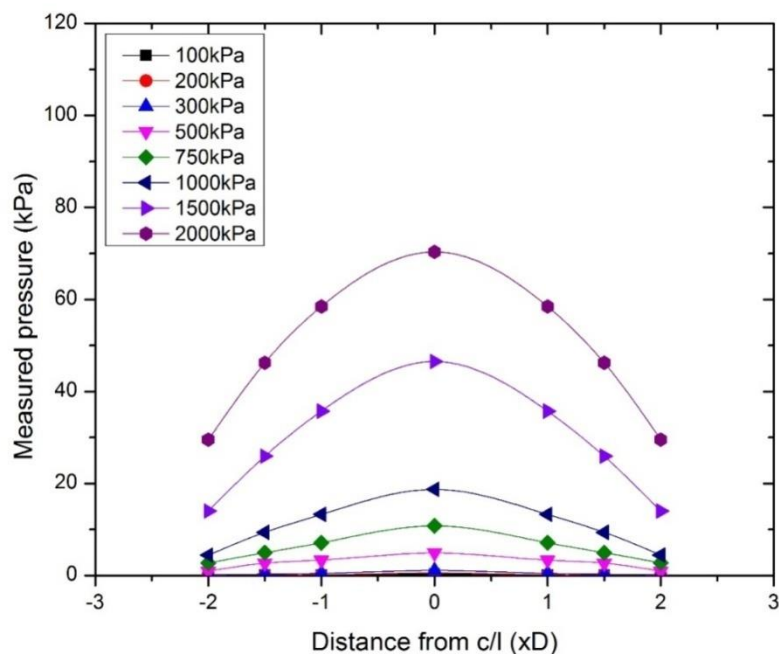


Figure 4.9 Pressure acting on the subgrade at different loads applied (Unreinforced)



Similarly, Fig. 4.10 presents the pressure distribution pattern at the subgrade level for various intensities of load applied on the geocell reinforced test section. It can be observed that there is an increase in the pressure intensities recorded with an increase in the applied pressure. However, the pressure distribution patterns in the reinforced section is observed to be less narrow, unlike the pressure distribution patterns of unreinforced section.

From the Fig. 4.9 and Fig. 4.10, it can be visualized that the pressure experienced at the subgrade level at all the specified locations is less in reinforced pavement section than the unreinforced section. It indicates that the geocell reinforcement is capable of distributing the loads to a wider area which in turn helps in reducing the pressure intensities observed at the subgrade level. About a 30% reduction in the pressure was observed in the geocell reinforced test sections compared to the unreinforced test sections at an applied pressure of 2000 kPa.



**Figure 4.10 Pressure acting on the subgrade at different loads applied (Reinforced 250 mm base)**

## 4.5 Repetitive load test results

During the second stage, repeated load tests were performed on the unreinforced and geocell reinforced test sections as listed in Table 4.5. The repeated loads are applied in such a way that it replicates the live traffic condition in the laboratory i.e. a traffic load equivalent to a contact pressure

of 550kPa. The performance of geocell reinforced test sections were compared w.r.t the control section and the performance indicators such as traffic benefit ratio (TBR), rut depth reduction (RDR), cumulative permanent deformations (CPD) and rut benefit ratio (RBR) were estimated for the geocell reinforced test sections.

In a repeated load test, there are two types of settlements observed in the pavement section i.e. elastic settlement which is ultimately regained on unloading and the other one is plastic settlement which cannot be regained, also called as permanent settlement. The summation of these plastic settlements after each loading cycle is called as cumulative plastic deformation (CPD). The variation of CPD with number of load cycles is presented in Fig. 4.11. Initially, it is observed that both the pavements are behaving same till 1000 load cycles, however, as the cycle number increases the difference in settlement increases between the two test sections. At 20,000 cycles, the deformation observed in unreinforced pavement section is around 2 mm with respect to the 1.85 mm deformation in reinforced case. At 1,00,000 cycles the reinforced pavement section settles only 2.71 mm compared to 3.11 mm in unreinforced case.

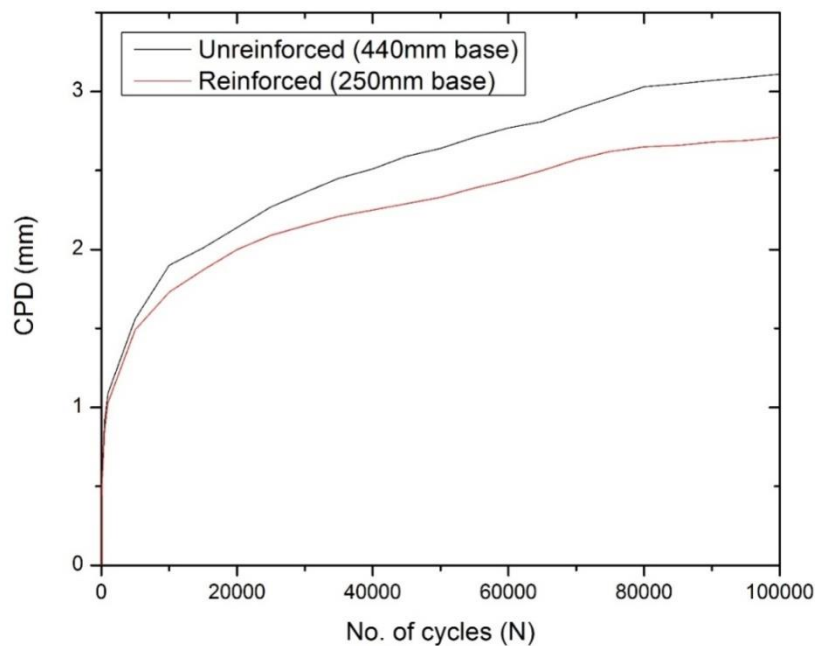


**Figure 4.11 Variation of cumulative plastic deformations with no. of load repetitions**

To quantify the amount of improvement, non-dimensional terms are used such as traffic benefit ratio (TBR), rut depth reduction ratio (RDR) and rut benefit ratio (RBR) graphs of which are shown in Fig.4.12, 4.13 and 4.14, respectively.

### 4.5.1 Traffic benefit ratio

Figure 4.12 shows variation of TBR with respect to CPD. As mentioned in section 3.7.2, the traffic benefit ratio (TBR) is a non-dimensional term used to quantify the benefits of the geo-synthetics used in pavement. It directly relates with the extension of life and also with savings in height of the base layer. As higher is the TBR value more will be its life. From the above Fig. 4.12, it is clearly seen that the TBR is increasing with the increase in CPD. A TBR of 1.7 indicates that the reinforced section will withstand till 1.7 times of designed load repetitions for unreinforced case i.e. 3.4msa in reinforced case at the same amount of settlement.

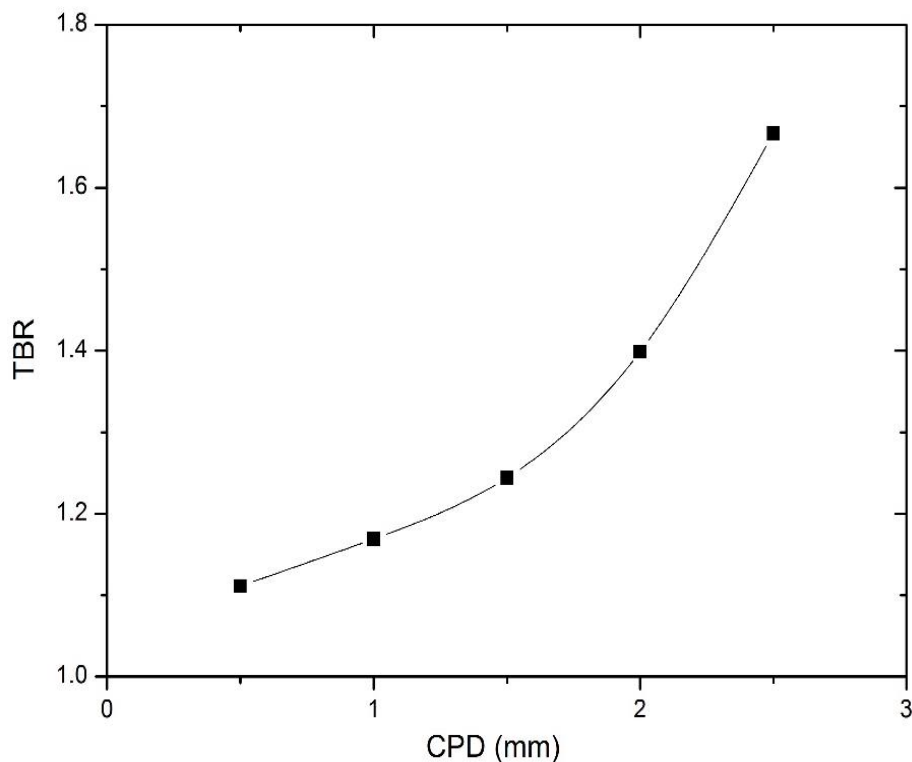


**Figure 4.12 Variation of TBR with CPD**

### 4.5.2 Rut depth reduction

It is a parameter used to quantify the pavement performance in terms of reduction in rut depth. From Fig. 4.13, it can be seen that initially the curve is steeper which changed to flattened after 80000 load cycles, it means that the reduction rate is higher initially and keeps on decreasing as the increase in number of loading cycles. It is a term which directly quantifies the reduction in rut by introducing the geocells in base layer. The rut depth reduction (RDR) is observed to be around 13% after the inclusion of the geocell in base layer, which means that the geocell helps in reducing the rut which ultimately helps in maintaining the evenness in level at top indicates good quality surface in reinforced roads.

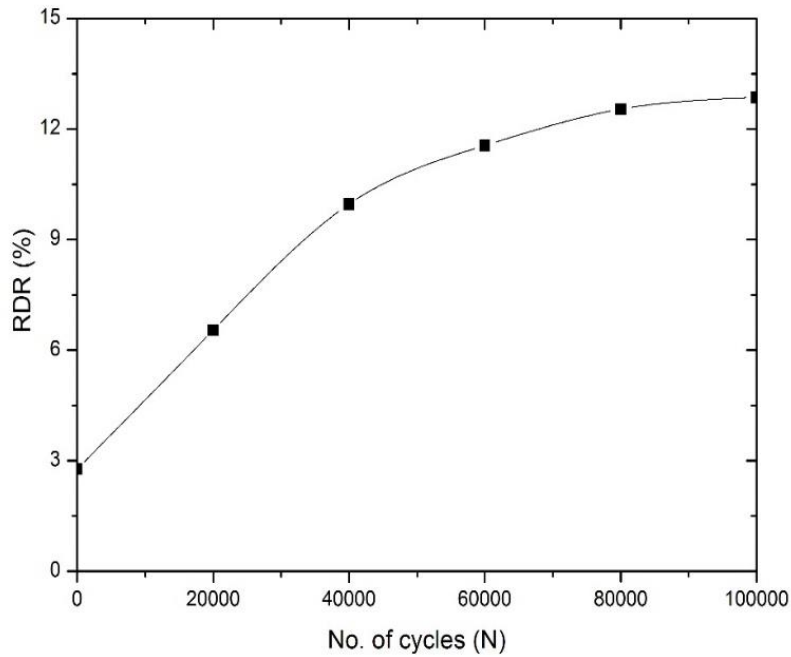


**Figure 4.13 Variation of RDR with number of loading cycles**

### **4.5.3 Subgrade deformation**

The subgrade deformation results in the deformation of layers above including the surface layer, forming a rut under the traffic wheel loads. To record the subgrade deformations and to understand the actual rut behavior at the subgrade level, an assembly consisting of two metal plates and a steel pipe is employed. The subgrade deformations recorded at different number of load cycles in both unreinforced and geocell reinforced test sections have been presented in Fig. 4.14. It can be observed that the geocell reinforced test sections have a less rut depth compared to the unreinforced test section at the same load cycles. It can be inferred that the geocell reinforcement in the base layers have reduced the rut depth at the subgrade level effectively. Further, the benefit in rut depth reductions are explained in the following section.

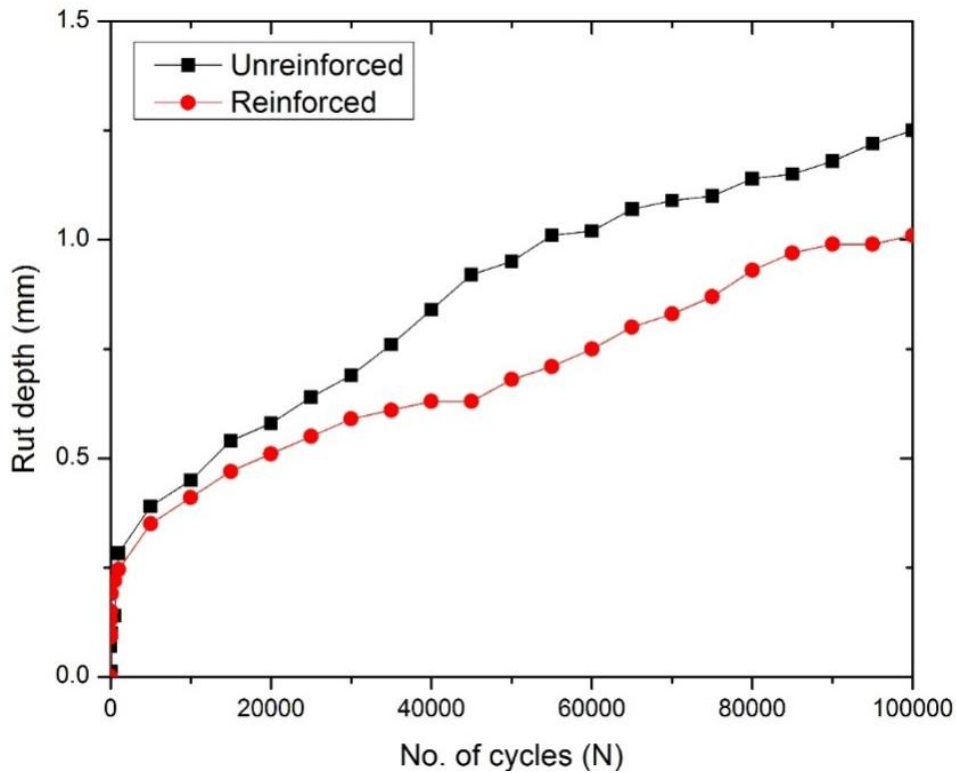


**Figure 4.14** Variation of rut depth with number of load cycles

#### 4.5.4 Rut benefit ratio

A new term, rut benefit ratio (RBR) is introduced in this study to evaluate the improvements in the rut depth reductions obtained at the subgrade level. The RBR is similar to RDR, as in both the terms quantifies the reduction in rut. Unlike similarities of the approach of finding, the major difference is that it gives the information about the rut directly at the subgrade which is not in case of RDR as it shows the improvement on the surface. The rut benefit ratio is as high as 20% in case of reinforced test sections as witnessed from Fig. 4.15.

As discussed in section 4.3, the test sections were instrumented with LVDTs and earth pressure cells for repetitive load tests and the instrumentation results are analyzed to understand the surface deformation profile and the vertical stress acting on the subgrade at different load cycles.

Figures. 4.16 and 4.17 presents the surface deformation profile for unreinforced and reinforced cases respectively. From Fig. 4.16 and Fig. 4.17, it is observed that up to 1000 cycles both are behaving almost same but as the number of load cycles increase, there is more settlement observed at the surface in unreinforced case. It is also observed that at the farthest location from the loading area, the deformation is seen minimal compared to the line of application of loads. The deflection basin in case of geocell reinforced test section is shallower, which indicates that the geocell helps in increasing the stiffness of the layer in which the geocells are introduced.

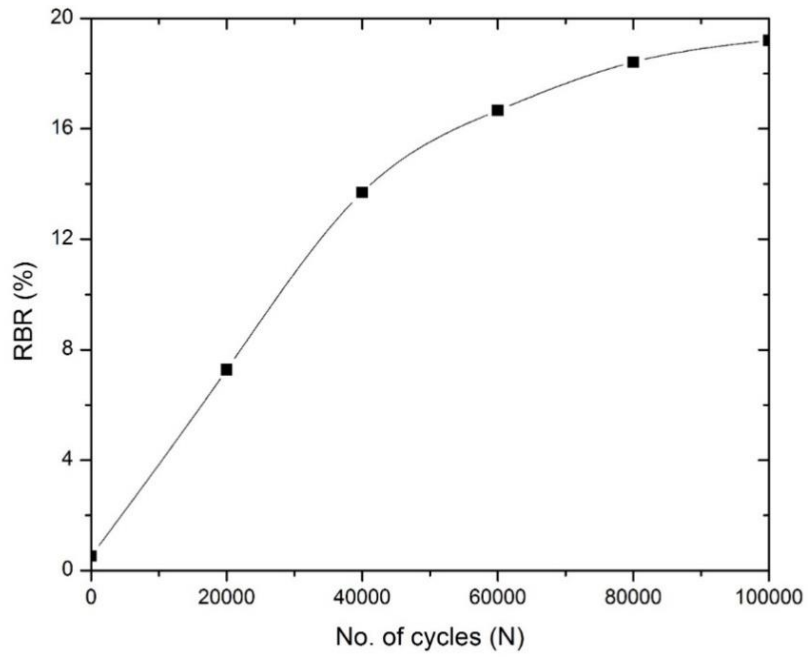


Figure 4.15 Variation of RBR with number of cycles

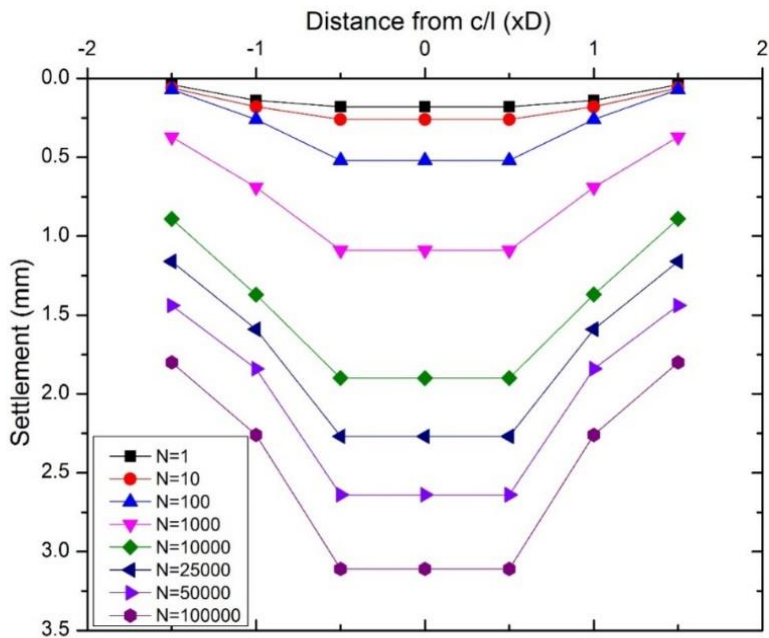
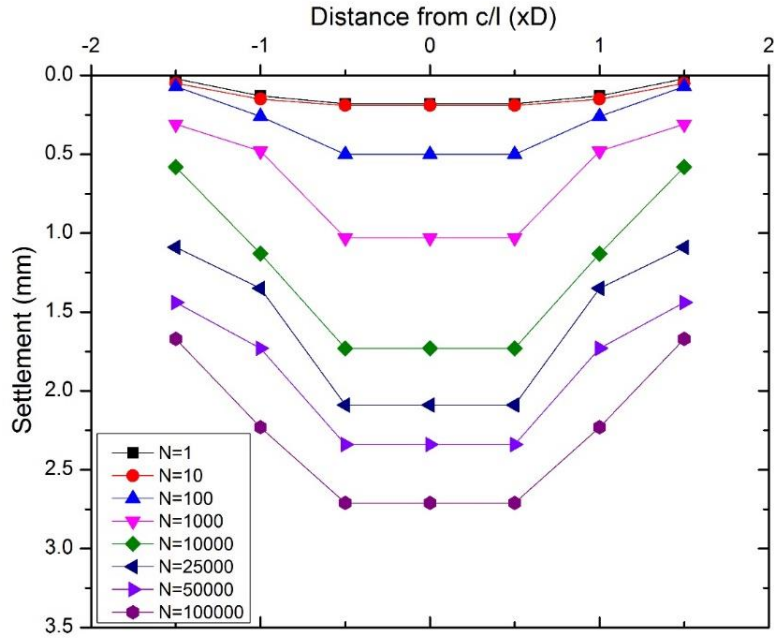


Figure 4.16 Surface deformation profile for unreinforced case



**Figure 4.17 Surface deformation profile of reinforced test section (250mm)**

The pressure acting on the subgrade with the applied pressure on the surface of the test sections is recorded with the help of the earth pressure cells installed similarly as in case of static loading test to understand the pressure distribution patterns. Figures. 4.18 and 4.19 presents the pressure distribution curves for unreinforced and reinforced case respectively. The pressure distribution curve gets sharper with an increase in number of loading cycles i.e. the pressure recorded exactly below the loading region is high. However, the pressure acting at a distance of 1D, 1.5D and 2D are relatively less.

It can be observed that there is an increase in the pressure intensities recorded with an increase in number of loading cycles, it is because of the reason that initially there are chances of settlement in the base layer because of the load applied but as the loading cycles increased further there is less chance of settlement in base layer and more load is transferred to the subgrade. However, the pressure distribution patterns in the reinforced section is observed to be less narrow, unlike the pressure distribution patterns of unreinforced section. It can also be visualized that the pressure experienced at the subgrade level at all the specified locations is less in reinforced pavement than the unreinforced. It indicates that the geocell reinforcement is capable of distributing the loads to a wider area which in turn helps in reducing the pressure intensities observed at the subgrade level. About a 20% reduction in the pressure was observed in the geocell reinforced test sections compared to the unreinforced test sections after 100000 loading cycles.

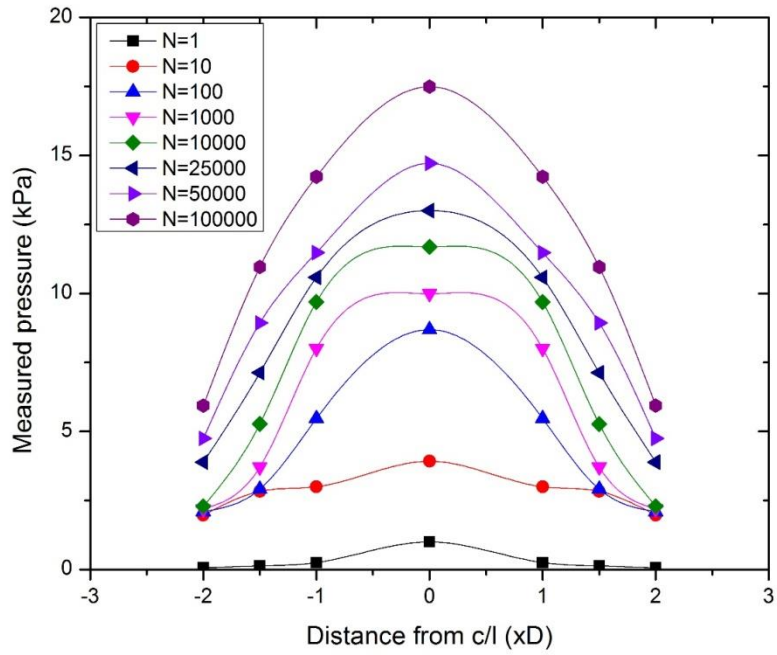


**Figure 4.18** Variation of contact pressure measured at the base-subgrade interface for geocell reinforced test section (250mm)

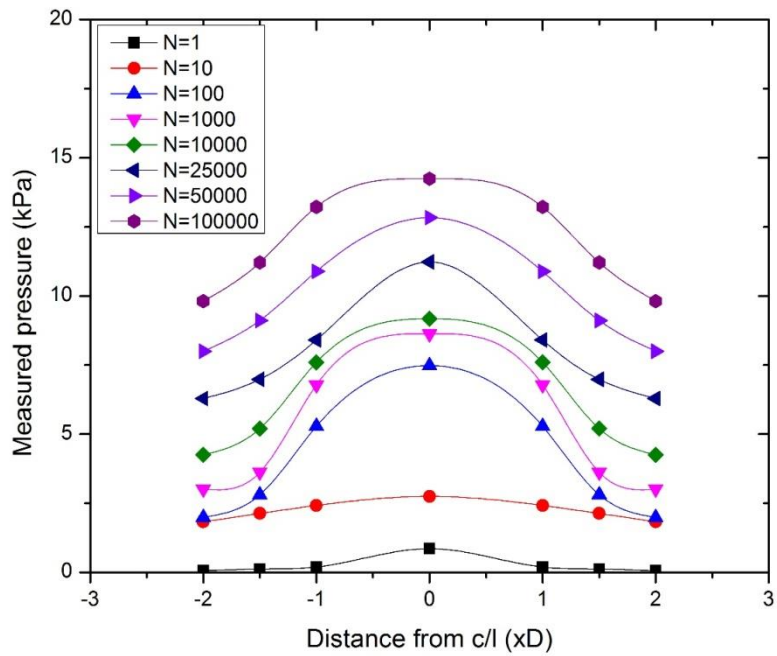


**Figure 4.19** Variation of contact pressure measured at the base-subgrade interface for geocell reinforced test section (250 mm)



## 4.6 Cost analysis

A detailed cost analysis has been carried out for the unreinforced geocell reinforced pavement sections. The cost of the granular base and bituminous layer are taken from the SOR for roads and bridge works of GOI. The cost analysis is carried out for two different test sections of a single lane flexible pavement and the results are tabulated in Tables 4.6 and 4.7 respectively. It can be seen that a net savings of Rs. 5,20,000 can be accounted for a km of reinforced flexible pavement section than the unreinforced pavement section. A reduction of about 10.15% were observed in the construction cost of a km stretch of flexible pavement.

**Table 4.6 Cost analysis of a km stretch of unreinforced flexible pavement**

S.No	Description of items	Length (m)	Width (m)	Thickness (m)	Quantity of material (m <sup>3</sup> )	Rate per unit	Price (Rs.)
1.	Wet Mix Macadam	1000	4	0.44	1760	2000/m <sup>3</sup>	35,20,000
2.	Bituminous layer	1000	4	0.05	200	8000/m <sup>3</sup>	16,00,000
3.	Total						51,20,000

**Table 4.7 Cost analysis of a km stretch of geocell reinforced flexible pavement**

S.No	Description of items	Length (m)	Width (m)	Thickness (m)	Quantity of material	Rate per unit	Price (Rs)
1.	Wet Mix Macadam	1000	4	0.25	1000 m <sup>3</sup>	2000/m <sup>3</sup>	20,00,000
2.	Bituminous layer	1000	4	0.05	200 m <sup>3</sup>	8000/m <sup>3</sup>	16,00,000
3.	Geocell material	1000	4		4000 m <sup>2</sup>	250/ m <sup>2</sup>	10,00,000
4.	Total						46,00,000

## 4.7 Summary

In this chapter, the results of the experiments conducted is discussed and is briefly explained the behavior of the pavement sections with and without reinforcement. The performance in terms of TBR, RDR, RBR and also the cost analysis of both the pavement section is discussed.

# Chapter 5

## Conclusion

For any civil engineering construction, the first and foremost thing to be kept in mind is cost. After comparing the cost analysis discussed in previous chapter, it clearly shows that reinforced pavement is 10.15% cheaper than the unreinforced pavement for every km single lane road construction. The inclusion of geocell in base layer results in reducing the base thickness to 43% to that of the unreinforced one, which ultimately reduces the usage of the virgin material which is very scarce in nature. The geocell also helps in reducing the permanent deformations of the pavement by inducing additional elasticity to the respective layers. The reduction in cumulative permanent deformation observed is 13% in reinforced case. Rut depth reduction (RDR) and rut benefit ratio (RBR) observed is 13% and 19% respectively, it indicates that the geocell helps in transferring the load to a larger area which ultimately induces less rut at subgrade. The equivalent modulus improvement factor observed is 1.3 times of the unreinforced pavement section which indicates that the reinforced pavement section is stiffer than the unreinforced one and that too with the reduced thickness. A TBR of 1.7 is achieved at only 50% of permissible settlement (5 mm) after applying 5% of designed traffic, it means that for the same settlement the reinforced pavement can sustain for a longer duration as compared to unreinforced one. A layer coefficient ratio of 1.82 is observed. This study finally concludes that the geocell reinforced pavement section of reduced thickness (250 mm base thickness) performs better than the unreinforced pavement section of base thickness 440 mm in all respects.

According to AASHTO, the thickness of unreinforced pavement section is 553 mm in place of 440 mm from IRC for the same traffic repetitions. The Indian roads are designed based upon IRC guidelines, which may result in premature failures due to the reason, that the correlations to calculate the resilient modulus of base layer, mentioned in IRC depends only on CBR of subgrade and does not consider resilient modulus of the layer itself. Whereas, in the case of AASHTO, the resilient modulus of individual layers are determined and designed as per the actual values obtained, unlike IRC method.

# References

- [1] <https://en.wikipedia.org/wiki/Geo-synthetics>, accessed on 20/06/2017.
- [2] Webster, S. L. (1981). Investigation of Beach Sand Trafficability Enhancement Using Sand-Grid Confinement and Membrane Reinforcement Concepts. Report 2. Sand Test Sections 3 and 4(No. WES/TR/GL-79-20). ARMY ENGINEER WATERWAYS EXPERIMENT STATION VICKSBURG MS GEOTECHNICAL LAB.
- [3] Carter, G. R. and Dixon, J. H. (1995). Oriented polymer grid reinforcement. *Construction and Building Materials*, 9(6), 389-401
- [4] Biabani, M. M., Ngo, N. T., and Indraratna, B. (2016). Performance evaluation of railway subballast stabilised with geocell based on pull-out testing. *Geo-textiles and Geomembranes*, 44(4), 579-591.
- [5] Kim, Y. J., Jo, S. H., Lee, S. H., & Kim, N. (2013). Field Applications on Environment-Friendly Permeable Pavements Reinforced by Geocell. *Journal of Korean Society of Hazard Mitigation*, 13(2), 143-149.
- [6] Giroud, J. P., and Noiray, L. (1981). Geo-textile-reinforced unpaved road design. *Journal of Geotechnical and Geoenvironmental Engineering*, 107. (ASCE 16489).
- [7] Barker, W. R. (1987). Open-Graded Bases for Airfield Pavements (No. WES/MP/GL-87-16). ARMY ENGINEER WATERWAYS EXPERIMENT STATION VICKSBURG MS GEOTECHNICAL LAB.
- [8] Haas, R., Walls, J., & Carroll, R. G. (1988). Geo-grid reinforcement of granular bases in flexible pavements (No. 1188). TRB, National Research Council, Washington, DC, USA, 19-27.
- [9] Al-Qadi, I. L., Brandon, T. L., Valentine, R. J., Lacina, B. A., & Smith, T. E. (1994). Laboratory evaluation of geo-synthetic-reinforced pavement sections. *Transportation Research Record*, (1439).
- [10] Bush D.I., Jenner C.G. and Besset R.H. The design and construction of geocell foundation mattress supporting over soft grounds, *Geo-textiles and Geomembranes*, Vol. 9, (1990) 83-98.
- [11] Barksdale, R. D., Brown, S. F., & Chan, F. (1989). Potential benefits of geo-synthetics in flexible pavement systems (No. 315).
- [12] Cowland, J. W., & Wong, S. C. K. (1993). Performance of a road embankment on soft clay supported on a geocell mattress foundation. *Geo-textiles and Geomembranes*, 12(8), 687-705.
- [13] Cancelli, A., & Cazzuffi, D. (1987). Permittivity of geo-textiles in presence of water and pollutant fluids. In *Proceedings of Geo-synthetics*, Vol. 87, pp. 471-481.

- [14] Collin, J. G., Kinney, T. C., & Fu, X. (1996). Full scale highway load test of flexible pavement systems with geo-grid reinforced base courses. *Geo-synthetics International*, 3(4), 537-549.
- [15] Dash, S. K., Krishnaswamy, N. R., and Rajagopal, K. (2001). Bearing capacity of strip footings supported on geocell-reinforced sand. *Geo-textiles and Geomembranes*, 19(4), 235-256.
- [16] Sitharam, T. G., & Sireesh, S. (2005). Behavior of embedded footings supported on geo-grid cell reinforced foundation beds, 452-463.
- [17] Saride, S., Pradhan, S., Sitharam, T. G., & Puppala, A. J. (2013). Numerical analysis of geocell reinforced ballast overlying soft clay subgrade. *Geomechanics and Engineering*, 5(3), 263-281.
- [18] Han J, Yang XM, Leshchinsky D, Parsons RL. Behavior of geocell-reinforced sand under a vertical load. *Transportation Research Board J*, (2008) No. 2045:95-101
- [19] Dash, S. K., Sireesh, S., & Sitharam, T. G. (2003). Model studies on circular footing supported on geocell reinforced sand underlain by soft clay. *Geo-textiles and Geomembranes*, 21(4), 197-219.
- [20] Mandal, J. N., & Gupta, P. (1994). Stability of geocell-reinforced soil. *Construction and building materials*, 8(1), 55-62.
- [21] Mhaikar, S.Y., Mandal, J.N., 1994. Three dimensional geocell structure: performance under repetitive loads. *Proceedings of the 5th International Conference on Geo-textiles, Geomembranes, and Related Products*, Singapore, pp. 155e158.
- [22] Rajagopal, K., Krishnaswamy, N.R., and Latha, G.M. Behavior of sand confined with single and multiple geocells. *Geo-textiles and Geomembranes*, (1999) 17(3), 171-184.
- [23] Hegde, A., & Sitharam, T. G. (2013). Experimental and numerical studies on footings supported on geocell reinforced sand and clay beds. *International Journal of Geotechnical Engineering*, 7(4), 346-354.
- [24] Halliday, A. R., & Potter, J. F. (1984). The performance of a flexible pavement constructed on a strong fabric. *TRRL LABORATORY REPORT*, (1123).
- [25] Mengelt, M., Edil, T. B., & Benson, C. H. (2006). Resilient modulus and plastic deformation of soil confined in a geocell. *Geo-synthetics International*, 13(5), 195-205.
- [26] Pokharel, S. K., Han, J., Parsons, R. L., Qian, Y., Leshchinsky, D., & Halahmi, I. (2009, June). Experimental study on bearing capacity of geocell-reinforced bases. In *8th international conference on Bearing Capacity of Roads, Railways and Airfields* (pp. 1159-1166). June 2009: Champaign, IL, USA.

- [27] Tafreshi, S. M., & Dawson, A. R. (2010). Comparison of bearing capacity of a strip footing on sand with geocell and with planar forms of geo-textile reinforcement. *Geo-textiles and Geomembranes*, 28(1), 72-84.
- [28] Pokharel, S. K., Han, J., Manandhar, C., Yang, X., Leshchinsky, D., Halahmi, I. & Parsons, R. L. (2011). Accelerated pavement testing of geocell-reinforced unpaved roads over weak subgrade. *Transportation Research Record*, 2204, 67–75.
- [29] American Association of State Highway, & Transportation Officials. (1993). *AASHTO Guide for Design of Pavement Structures*, 1993 (Vol. 1). AASHTO.
- [30] Korulla, M., Gharpure, A., & Rimoldi, P. (2015). Design of geo-grids for road base stabilization. *Indian Geotechnical Journal*, 45(4), 458-471.
- [31] Technical Note: "Development of Geo-grid Reinforced Flexible Pavement Layer Coefficient Ratios (LCRs) Based on FullScale Trafficking Trials." Available at [www.bostd.com](http://www.bostd.com).
- [32] IS 2720(PART4-1985) Methods of test for soils: Sieve analysis of soil
- [33] IS-2720 (Part4-1972) Methods of test for soils: Atterberg's limit of soil.
- [34] IS-2720 (Part3-1980) Methods of test for soils: Specific gravity of soil.
- [35] IS-2720 (Part7-1980) Methods of test for soils: Standard compaction test on soil.
- [36] IS 2720 (PART-16) 1987 Methods of test for soils: laboratory Determination of CBR
- [37] MORTH specification, 406.2.1.2. (Table 400-11) 2000, Grading requirements of WMM.
- [38] IS-2720 (Part8-1980) Methods of test for soils: Modified compaction test on soil.
- [39] Edil, T. B., Kim, W. H., Benson, C. H., & Tanyu, B. F. (2007). Contribution of geo-synthetic reinforcement to granular layer stiffness. In *Soil and Material Inputs for Mechanistic-Empirical Pavement Design* (pp. 1-10).
- [40] Indian Road Congress, (2012). *Guidelines for the design of flexible pavements. Indian code of practice, IRC-37*, New Delhi.
- [41] American Association of State Highway, & Transportation Officials. (2009). *AASHTO Standard Practice for Geo-synthetic Reinforcement of the Aggregate Base Course of Flexible Pavement Structures*, AASHTO.
- [42] Krishnaswamy, N. R., Rajagopal, K., & Latha, G. M. (2000). Model studies on geocell supported embankments constructed over a soft clay foundation.
- [43] Sireesh S. Behavior of Geocell Reinforced Foundation Beds Ph. D. Thesis, Indian Institute of science, Bangalore, 2005.
- [44] Tafreshi, S. M., & Dawson, A. R. (2012). A comparison of static and cyclic loading responses of foundations on geocell-reinforced sand. *Geotextiles and Geomembranes*, 32, 55-68.
- [45] Yang, X., Han, J., Pokharel, S. K., Manandhar, C., Parsons, R. L., Leshchinsky, D., & Halahmi, I. (2012). Accelerated pavement testing of unpaved roads with geocell-reinforced sand bases. *Geotextiles and Geomembranes*, 32, 95-103.